NAVAL POSTGRADUATE SCHOOL
Monterey, California

THESIS

A STUDY OF THE MICROSTRUCTURAL BASIS FOR THE STRENGTH AND TOUGHNESS PROPERTIES OF AS-QUENCHED AND QUENCHED AND TEMPERED HIGH COPPER HSLA-100 STEEL

by

Harvey Allen Winters

DECEMBER 1991

Thesis Advisor: Alan G. Fox

Approved for public release: Distribution is unlimited

Unclassified

SECURITY CLASSIFICATION OF THIS PAGE

REPORT DOCUMENTATION PAGE

Form Approved OMB No 0704-0188

1a. REPORT SECURITY CLASSIFICATION: Unclassified	1b. RESTRICTIVE MARKINGS
2a. SECURITY CLASSIFICATION AUTHORITY	3. DISTRIBUTION/AVAILABILITY OF REPORT: Approved for public release: Distribution is unlimited
2b. DECLASSIFICATION/DOWNGRADING SCHEDULE	
4. PERFORMING ORGANIZATION REPORT NUMBER(S)	5. MONITORING ORGANIZATION REPORT NUMBER(S)
6a. NAME OF PERFORMING ORGANIZATION: Naval Postgraduate School; 6b. OFFICE SYMBOL (If applicable): ME	7a. NAME OF MONITORING ORGANIZATION: Naval Postgraduate School
6c. ADDRESS (City, State and ZIP Code): Monterey, CA 93943-5000	7b. ADDRESS (City, State, and ZIP Code): Monterey, CA 93943-5000
8a. NAME OF FUNDING/SPONSORING ORGANIZATION; 8b. OFFICE SYMBOL (If applicable)	9. PROCUREMENT INSTRUMENT IDENTIFICATION NUMBER
8c. ADDRESS (City, State, and ZIP Code)	10. SOURCE OF FUNDING NUMBER: PROGRAM ELEMENT NO. / PROJECT NO. / TASK NO. / WORK UNIT ACCESSION NO.

11. TITLE (Include Security Classification)
A STUDY OF THE MICROSTRUCTURAL BASIS FOR THE STRENGTH AND TOUGHNESS PROPERTIES OF AS-QUENCHED AND QUENCHED AND TEMPERED HIGH COPPER HSLA-100 STEEL

12. PERSONAL AUTHORS
HARVEY ALLEN WINTERS

13a. TYPE OF REPORT	13b. TIME COVERED	14. DATE OF REPORT (Year, Month, Day)	15. PAGE COUNT
Master's Thesis	FROM_____ TO_____	DECEMBER 1991	78

16. SUPPLEMENTARY NOTATION
The views expressed are those of the author and do not reflect the official policy or position of the Department of Defense or the U.S. Government

17. COSATI CODES			18. SUBJECT TERMS (Continue on reverse if necessary and identify by block numbers)
FIELD	GROUP	SUB-GROUP	high copper HSLA-100 steel

19. ABSTRACT (Continue on reverse if necessary and identify by block numbers)

A program for the use of high copper HSLA-100 steel as a replacement for HY-130 in ship construction is in progress at the David Taylor Naval Research Center in Annapolis, Maryland. The characterization of the microstructure of this highly weldable high copper HSLA-100 steel is extremely important to this program. In the present work, optical, scanning electron and transmission electron microscopy were employed to analyze and characterize the microstructural basis for the mechanical properties off as-quenched and quenched and tempered high copper HSLA-100 steel in the form of 19.05 mm plate. The as-quenched and samples aged at 538°C and 621°C were examined in great detail. In the as-quenched condition the microstructure consisted of small packets of highly dislocated lath martensite containing autotempered Fe_3C carbides with small amounts of retained austenite present as thin films (200-300 Å in width) at lath boundaries. **CONTINUED ON NEXT PAGE**

20. DISTRIBUTION/AVAILABILITY OF ABSTRACT	21. ABSTRACT SECURITY CLASSIFICATION
XX UNCLASSIFIED/UNLIMITED __ SAME AS RPT __ DTIC USERS	unclassified

22a. NAME OF RESPONSIBLE INDIVIDUAL	22b. TELEPHONE (Include Area Code)	22c. OFFICE SYMBOL
Alan G. Fox	(408) 646-2142	ME/Fx

DD Form 1473, JUN 86 — Previous editions are obsolete. S/N 0102-LF-014-6603

Continued from BLOCK 19

The basis for the high strength and toughness of this as-quenched sample is the small transformation product packet size and the highly dislocated structure. The best combination of strength and toughness occurred in the sample aged at 538°C. Contributing to these desirable characteristics was the recovery of the dislocation substructures, the precipitation of coherent BCC copper precipitates (12-20 Å in size) further precipitation $(FeM)_3C$ carbides and the small transformation product packet size. In the overaged (621°C) condition, the toughness was increased and the strength decreased due to the absence of coherent BCC. copper precipitates and the presence of FCC ε-copper incoherent precipitates. Further recovery of the dislocation substructures was also evident. All of the samples (lot GLB) studied met the MILSPEC for HY-130 and would be suitable replacements. As a result of this investigation it is suggested that the optimum aging temperature for the 19.05 mm as-quenched high copper HSLA-100 plate is around 550°C.

Approved for public release: Distribution is unlimited

A Study of the Microstructural Basis for the Strength and Toughness Properties of As-Quenched and Quenched and Tempered High Copper HSLA-100 Steel

by

Harvey Allen Winters
Lieutenant, United States Navy
B.S.N.A., United States Naval Academy, 1986

Submitted in partial fulfillment of the requirements for the degree of

MASTER OF SCIENCE
IN MECHANICAL ENGINEERING

from the

NAVAL POSTGRADUATE SCHOOL

DECEMBER 1991

Author: Harvey Allen Winters
Harvey Allen Winters

Approved by: A. G. Fox
Alan G. Fox, Thesis Advisor

A.J. Healey, Chairman
Department of Mechanical Engineering

ABSTRACT

A program for the use of high copper HSLA-100 steel as a replacement for HY-130 in ship construction is in progress at the David Taylor Naval Research Center in Annapolis, Maryland. The characterization of the microstructure of this highly weldable high copper HSLA-100 steel is extremely important to this program. In the present work, optical, scanning electron and transmission electron microscopy were employed to analyze and characterize the microstructural basis for the mechanical properties off as-quenched and quenched and tempered high copper HSLA-100 steel in the form of 19.05 mm plate. The as-quenched and samples aged at 538°C and 621°C were examined in great detail. In the as-quenched condition the microstructure consisted of small packets of highly dislocated lath martensite containing autotempered Fe_3C carbides with small amounts of retained austenite present as thin films (200-300 Å in width) at lath boundaries. The basis for the high strength and toughness of this as-quenched sample is the small transformation product packet size and the highly dislocated structure. The best combination of strength and toughness occurred in the sample aged at 538°C. Contributing to these desirable characteristics was the recovery of the dislocation substructures, the precipitation of coherent BCC copper precipitates (12-20 Å in size) further precipitation $(FeM)_3C$ carbides and the small transformation product packet size. In the overaged (621°C) condition, the toughness was increased and the strength decreased due to the absence of coherent BCC copper precipitates and the presence of FCC ε-copper incoherent precipitates. Further recovery of the dislocation substructures was also evident. All of the samples (lot GLB) studied met the MILSPEC for HY-130 and would be suitable replacements. As a result of this investigation it is suggested that the optimum aging temperature for the 19.05 mm as-quenched high copper HSLA-100 plate is around 550°C.

TABLE OF CONTENTS

LIST OF TABLES

LIST OF FIGURES

I. INTRODUCTION

Modern naval warships are subjected to complex dynamic loadings and stresses during their life cycles. Designs of these warships need to continue to increase the use of high strength, low alloy steels for weight reduction, increased mobility and payload to provide ordnance on target. Ship structures are subjected to many stresses: fabrication, waveloading, mechanical vibrations, aircraft operation, weapons firing and detonation, cargo transfer, and many others. This complex system must be able to operate in extreme weather conditions [Ref. 1:pp. 1-2].

An equally important requirement in the design of warships is their ability to maintain their structural integrity. Therefore ships must meet highly stringent requirements in strength and toughness imposed by these "environmental" conditions. For these reasons, steel with high fracture toughness and flaw propagation tolerance must be utilized [Ref. 1:p. 2]. In addition to these requirements, fiscal constraint must also be addressed and satisfied [Ref. 2:p. 1].

The HY series of steels have been typically utilized in U.S. Naval Ship Construction. Though these steels satisfy most requirements, they are not easily weldable [Ref. 3:p. 26] and require many fabrication controls to prevent post-weld cracking and failure. In addition to these undesirable post-

weld effects, expensive fabrication costs, welder training costs and qualifications procedures are major concerns [Ref. 1:p. 2] in this period of shrinking defense budgets.

To reduce shipbuilding and repair costs, the U.S. Navy has started and maintained a research development certification program for High Strength Low Alloy (HSLA) steels. These steels use microalloying and thermomechanical processing to obtain desired mechanical properties [Ref. 3:p. 3]. Compared to the HY series of steels, HSLA steels exhibit excellent weld characteristics and are more resistant to hydrogen cracking [Ref. 4:p. 68]. This allows increased productivity and a cost reduction for shipyards [Ref. 5:pp. 21-26].

The HY series of steels are martensitic in microstructure, and rely upon a quench and temper treatment to attain the required strength and toughness. Unfortunately, high carbon levels adversely affect the weldability of the material and result in the need for fabrication controls. The newly developed HSLA series of steels, have shown that alloy steels can have good strength and toughness without high carbon levels. This reduction in carbon requires an increase in strength through other alloying agents such as copper and improved thermomechanical processing techniques. The toughness of these alloys results from thermo-mechanical processing, microalloying, and improved steelmaking cleanliness [Ref. 3:pp. 26-27] [Ref. 2:p. 2]. The use of HSLA steels has resulted in a significant reduction in hull fabrication costs,

increased productivity due to reduced process controls and NDT requirements, and is currently used as the primary structural steel in the Ticonderoga class cruisers, Arleigh Burke class destroyers, and the Nimitz class aircraft carrier USS John C. Stennis [Ref. 1:p. 3] [Ref. 2:p. 2].

The Navy has a continuing HSLA steels research and development program to produce low cost alternatives to the HY series of steels. The development of a new 130 ksi yield strength grade will take advantage of new technologies such as low carbon bainite, microalloying, copper strengthening, and clean steelmaking, as well as more traditional metallurgy to provide an easily produced, inexpensive HSLA-130 grade steel. [Ref. 3:p. 27] [Ref. 2:p. 3]. This thesis will investigate the microstructural basis for the strength and toughness properties of a high copper HSLA-100 steel which achieves the 130 ksi yield strength level.

II. BACKGROUND

A. INTRODUCTION TO HSLA STEELS

Approximately seven percent of all steels made in the United States are of the high strength low alloy variety; this percentage is expected to grow in the future [Ref. 6:p. 41]. This type of steel has a martensitic microstructure but does not have a high carbon level and still attains high levels of strength, toughness and desired hardenability. Advances in technology have allowed steels to be processed with low carbon content and a better understanding of the microalloying process has contributed to the increased utilization of HSLA steels [Ref. 7:p. 4].

Economics are also an important consideration in this time of shrinking defense budgets. Close matching of strength and other property requirements have realized cost savings of about 30% over plain carbon steels [Ref. 8:p. 17]. The amount of research invested (and also dollars) in HSLA steels has been large but not haphazard. It was based on planned, systematic research [Ref. 6:p. 41] [Ref. 9:p. 61]. This has led to the development of a strong, tough, and highly weldable steel. This can best be seen by the Graville diagram, Figure 1.

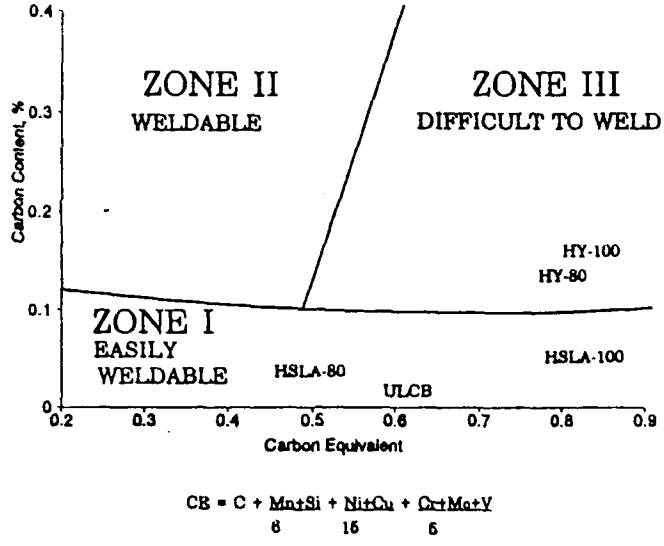

Figure 1 **The Graville Diagram: Influence of Carbon Level and Carbon Equivalent on Susceptibility to HAZ Cracking of Steel Plate. [Ref. 10:p. 183]**

Research in North America, Europe, and Japan concentrated on: 1) developing an understanding of the factors affecting grain size; 2) development of a better understanding of the strengthening mechanisms involved in steel and the relations between this type of strengthening and its influence on the ductile to brittle transition temperature; and 3) studying the effects of thermomechanical processing and composition and their influence on strength and toughness. [Ref. 8:p. 17]

The Navy is highly interested in the HSLA series of steels. HSLA-80 and HSLA-100 steels have been certified for use in ship construction. The HSLA series of steels are a

derivation of the ASTM-A710 commercial steel. The chemical composition of HSLA-100 steel according to MILSPEC MIL-S-24645A is listed in Table I [Ref. 11:p. 3].

TABLE I. HSLA-100 STEEL MIL-S-24645A COMPOSITION (WEIGHT PERCENT)

C	0.04-0.06
Mn	0.75-1.05
P	0.020
S	0.006
Si	0.40
Ni	3.35-3.65
Cr	0.45-0.75
Mo	0.55-0.65
Cu	1.45-1.75
Nb	0.02-0.06

HY steels attain their strength through quench and temper treatments, but HSLA steels achieve their strength through grain refinement, precipitation strengthening and solid solution strengthening [Ref. 12:p. 5-22]. Dislocation substructures also contribute to the strength of HSLA steels [Ref. 11:p. 3]. These strengthening mechanisms reduce dislocation mobility and increase the stress required to move these dislocations. [Ref. 13:p. 21].

B. REVIEW OF HSLA STEELS

ASTM-A710 steel was the commercial HSLA steel identified by DTRC as the prime candidate among commercial steels to replace the HY series of steels [Ref. 1:p. 2]. This steel is a low carbon, copper precipitated strengthened steel that can be welded without preheat in plate thickness up to 19.05 mm (0.75 in) [Ref. 11:p. 2]. In 1984, ASTM-A710 was renamed HSLA-80 by the Navy, given the designation MILSPEC MIL-S-24645 and certified for use in ship construction. [Ref. 2:p. 7]

A search began for an HSLA steel to replace HY-100. The Navy decided that a highly weldable, copper precipitation strengthened steel was the best option. This steel must be copper precipitation strengthened, contain niobium for grain size control, have a maximum carbon content of 0.07 weight percent, have a maximum sulfur content of 0.008 weight percent, and have a maximum phosphorous content of 0.010 weight percent. It must also contain manganese (Mn), chromium (Cr), nickel (Ni) and molybdenum (Mo). The steel should also be solution treated, quenched, and aged. In 1989, HSLA-100 was certified and designated MIL-S-24645A. Table II shows the chemical composition of the HY and HSLA steels. [Ref. 11:p. 2] [Ref. 1:pp. 3-4].

Grain refinement, solid solution and precipitation strengthening are some of the mechanisms responsible for the strength of HSLA steels. Each of these strengthening mechanisms decrease dislocation motion and increase the stress

TABLE II CHEMICAL COMPOSITION OF HIGH STRENGTH STRUCTURAL STEELS. (MAJOR ELEMENTS FOR HEAVY GAGE PLATE, GREATER THAN 1 INCH) [REF 1:P. 4] [REF. 2:P. 6]

Element (weight %)	Specified Chemical Composition (maximum unless a range is shown)			
	HY-80 MIL-S-16216K	HSLA-80 MIL-24645	HY-100 MIL-S-16216K	HSLA-100 MIL-S-24645A
C	0.13-0.118	0.06	0.14-0.20	0.06
Mn	0.10-0.40	0.40-0.70	0.10-0.40	0.75-1.05
P	0.015	0.020	0.015	0.020
S	0.008	0.006	0.008	0.006
Si	0.15-0.38	0.40	0.15-0.38	0.40
Ni	2.50-3.50	0.70-1.00	2.75-3.50	3.35-3.65
Cr	1.40-1.80	0.60-0.90	1.40-1.80	0.45-0.75
Mo	0.35-0.60	0.15-0.25	0.35-0..60	0.55-0.65
Cu	0.25	1.00-1.360	0.25	1.45-1.75
Nb	nil	0.02-0.06	nil	0.02-0.06

required to move these dislocations. These highly dislocated microstructures are a large contributor to the strength. [Ref. 7:p. 6]

Microalloying is one of the secrets to the high strength and toughness of the HSLA series of steels [Ref. 6:p. 41]. Alloy additions affect grain size, precipitation, solid solution strengthening and the development of dislocation substructures. Alloying (the addition of copper, mainly) moves the transformation region in the continuous cooling transformation (CCT) curves, altering austenitic transformation characteristics (Figure 2).

The metallurgical significance of alloying elements involved are listed below [Ref. 2:p. 12]

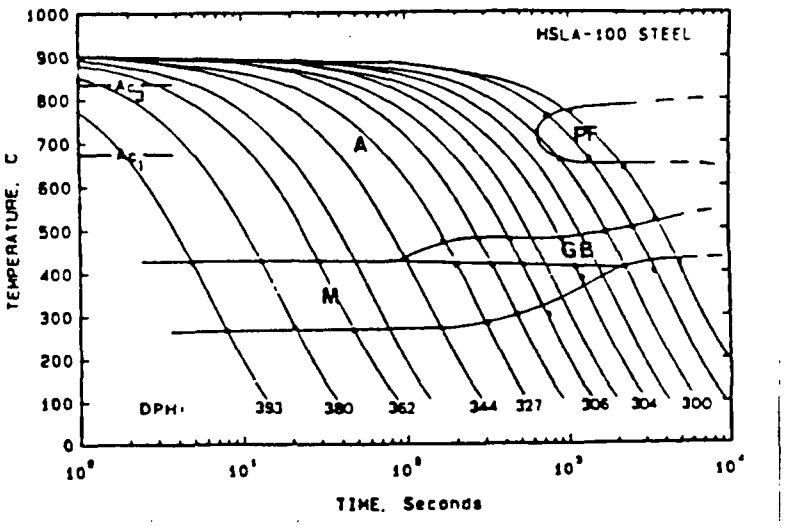

Figure 2 **HSLA-100 Steel Continuous Cooling Transformation Diagram. [Ref. 14:p. 262]**

- **Carbon** - Increases in carbon content improves the steel's ability to form martensite which increases strength. Carbon also is an excellent solid solution strengthener. Lower carbon content leads to improved toughness and a lower ductile-brittle transition temperature (DBTT) since fewer crack-initiating carbides exist. Low carbon concentrations also provide a highly weldable steel insensitive to hydrogen-induced cracking (HIC); the need for pre-heat can also be eliminated [Ref. 3:pp. 64-65.]

- **Manganese** - Reacts with sulfur to form MnS, preventing the formation of harmful FeS at grain boundaries which causes 'hot cracking.' Mn is also a good deoxidizer when combined with silicon [Ref. 15:p. 19] and lowers the DBTT and elevates strength when in solid solution. [Ref. 6:p. 376]

- **Copper** - Increases strength by precipitation of copper-rich particles during aging [Ref. 14:p. 260]. Improves corrosion resistance to seawater and reduces susceptibility to hydrogen induced cracking [Ref. 14:p. 67].

- **Nickel** - Increases strength by enhancing grain refinement and solid solution strengthening; Ni reduces the DBTT but does not affect Charpy upper shelf energy [Ref. 16:p.

391]. Prevents the hot shortness phenomenon associated with welding of steels containing copper. Dramatically increases hardenability and promotes higher toughness [Ref. 14:p. 260].

- **Niobium** - Combines with nitrogen and carbon to form niobium carbonitrides Nb(C,N) which provide grain refinement during hot rolling and later austenitizing treatment by pinning the austenite grain boundaries. Increases strength through carbide and nitride formation. [Ref. 14:p. 260]

- **Molybdenum** - Increases strength without loss in toughness. Strong carbide former, influences transformation kinetics by delaying the onset of proeutectoid ferrite formation; suppresses temper embrittlement. [Ref. 14:p. 260]

- **Vanadium** - Strong carbide and nitride former [Ref. 16:p. 376].

- **Silicon** - Excellent deoxidizer; prevents porosity during steelmaking. [Ref. 17:p. 8]

- **Chromium** - Increases hardenability of bainite by delaying onset of proeutectoid ferrite formation; retards tempering during aging; provides corrosion resistance; strong carbide former. [Ref. 14:p. 260] [Ref. 16:p. 376]

- **Aluminum** - Lowers DBTT by removing nitrogen from solid solution which lowers the lattice resistance to dislocation motion; strong deoxidizer. Forms AlN which pins grain boundaries and keep ferrite grain size small. [Ref. 6:p. 47] [Ref. 18:p. 9]

The addition of copper can also reduce the phenomenon of hydrogen-induced cracking. This type of cracking will normally begin at manganese sulfide (MnS) inclusions and will proceed in two modes: (1) straight cracking parallel to the rolling direction and (2) stepwise cracking. Copper treated steels containing low amounts of sulfur will show a decrease in the average crack length as copper content increases (Figure 3) [Ref. 14:p. 118-119]

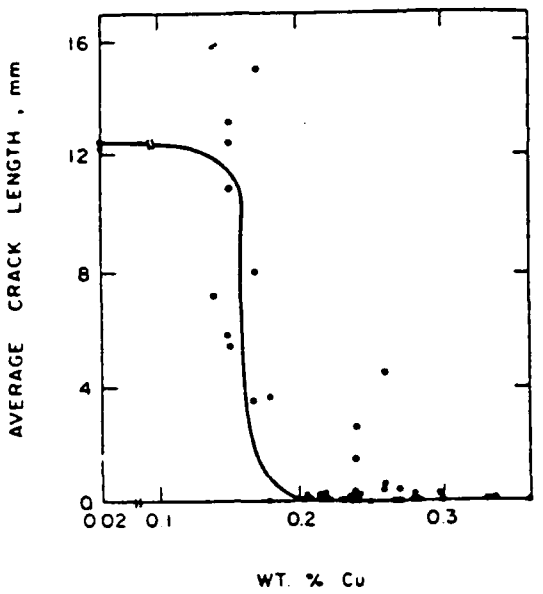

Figure 3 Effect of Copper on Average Hydrogen-Induced Crack Length. [Ref. 14:p. 120]

HSLA steels have a bainitic/martensitic microstructure. HSLA-80 and HSLA-100 have been determined to have a bainitic microstructure as previously reported by Mattes, Comerford, and Mohr [Ref. 18] [Ref. 7] [Ref. 2]. The strength of bainitic steels is due to four separate factors. [Ref. 2:p. 17]

- **Lath and packet size strengthening** - numerous studies have shown that lath width and bainite packet size affect strength; the flow stress usually varies with the reciprocal of some characteristic lath dimension. Pickering showed that the ferrite grain size (bainitic lath size) gives the usual Petch relationship with 0.2% proof stress (Figure 4). The lath dimensions decrease with decreasing transformation temperature.
- **Dislocation strengthening** - transformation strains induce a higher density of dislocations which increase strength. As transformation temperature decreases, the density of dislocations increases.

- **Interstitial and substitutional strengthening** - the carbon dissolved in the bainitic ferrite causes solid solution strengthening. Experimental evidence also shows a residual super-saturation of carbon atoms can interact with dislocations to increase the strength significantly.

- **Carbide strengthening** - In upper bainite the coarser particles at the lath boundaries impede dislocation motion but do not appear to affect the strength of the microstructure via dispersion strengthening. In lower bainite, the increased number of fine intralath carbides per unit planar section increases the proof stress [Ref. 9:p. 1112] [Ref. 2:p. 22]

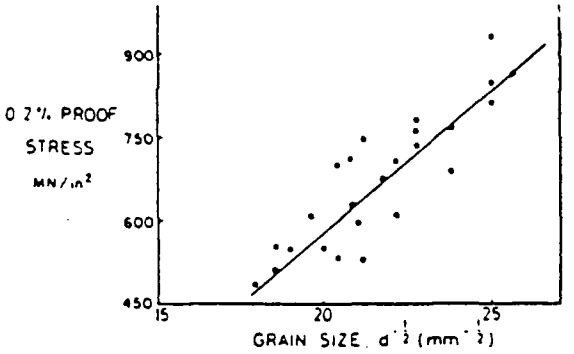

Figure 4 Effect of Ferrite Grain Size on 0.2% Proof Stress. [Ref. 9:p. 112]

High copper HSLA-100 is being investigated as a replacement for HY-130 steel. In the present work, it has been determined to have a highly dislocated martensitic microstructure. This martensitic microstructure is the major difference between high copper HSLA-100 and the previous HSLA steels. Even though high copper HSLA-100 has a martensitic microstructure, it is still a highly weldable steel.

For a HSLA replacement for HY-130, the Navy has decided that the additional strengthening must be derived through precipitation hardening. Dispersed precipitates generally increase strengthening by impeding dislocation motion through Orowan Looping [Ref. 13:pp. 21-22]. Coherent precipitation will cause the highest degree of hardening due to the coherency strain fields associated with their interface with the steel matrix. Those coherency strength fields will block dislocation motion leading to higher strength. Upon aging, these coherent precipitates become incoherent and their ability to block dislocation motion become reduced. Dislocation motion is now easier and the material's strength begins to decrease. [Ref. 19:pp. 319-324.]

Copper is a precipitation strengthener. It first precipitates coherently and then becomes incoherent upon aging. As shown by Figure 5, the maximum solubility of copper in iron is 2.1 weight percent. It can also be seen from figure 5 that copper's decreasing solubility provides a good opportunity for age hardening. Additional strengthening is also provided by niobium carbides and carbonitrides. [Ref. 20:p. 791]

Goodman, Brenner, and Low have studied the precipitation of copper in iron using field ion microscopy. They discovered that aging of the supersaturated Fe-Cu alloy resulted in precipitation of copper-rich BCC clusters that formed in ferrite. Maximum strength was attained during the

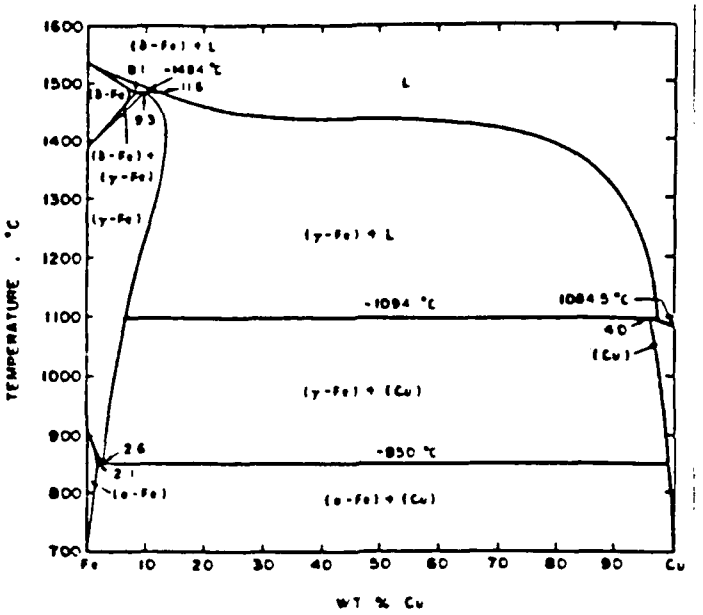

Figure 5 Fe-Cu Phase Diagram. [Ref. 13:p. 8]

precipitation of this coherent non-equilibrium phase while the precipitates were still B.c.c. During overaging, these clusters transform into larger face-centered cubic (FCC) equilibrium epsilon phase precipitates containing a larger amount of copper; their loss of coherency makes them visible in the transmission electron microscope [Ref. 21:p. 121]. The transformation from BCC to FCC relieves crystallographic strain [Ref. 22:p. 803]. The incoherent particles were found to be spherical and randomly distributed throughout the matrix; as aging continued, the precipitates became rod-shaped [Ref. 23:p. 624]. The density of precipitates remained nearly constant until peak strength was reached and then decreased during overaging. [Refs. 24, 25] [Ref. 7:pp. 20-21]

Although continued aging after peak hardness reduces the material's strength, it usually increases its toughness. The enhanced toughness of high copper HSLA-100 is due in large part to the overaged condition of the copper precipitates [Ref. 26:pp. 244-248]. The larger, incoherent copper particles localized slip and formation of dislocation pileups at grain boundaries thereby increasing the upper shelf fracture toughness [Ref. 22:p. 798] [Ref. 7:p. 22]

C. THE TEMPERING PROCESS

Tempering is now said to consist of five stages. These are:

Stage I. The formation of a transition carbide for steels with carbon content greater than 0.2 weight percent; epsilon carbide or eta carbide, and the lowering of the carbon content of the matrix martersite to about 0.25% carbon. [Ref. 27:p. 200]

Stage II. The transformation of retained austenite to bainitic ferrite and cementite. [Ref. 27:p. 200]

Stage III. The replacement of the transition carbide and low carbon martensite by cementite and ferrite. [Ref. 27:p. 200]

Stage IV. The precipitation of alloy carbides of the type $(FeM)_3C$ where M represents any of the carbide forming substitutional atoms present in the steel. This tempering process contributes to the strength of the steel due to the coherency of the precipitates. [Ref. 30:pp. 745-746]

Stage V. The replacement of cementite by alloy carbides producing a secondary hardening peak. [Ref. 28:p. 635] [Ref. 29:p. 9]

Another type of tempering is "auto-tempering" or "Q-tempering" as reported by Chilton and Kelly and Aborn [Ref. 31:p. 638] [Ref. 32:p. 69]. This type of tempering will occur in steels with high martensite start temperatures and thus a carbon content of less than 0.2 weight percent. The precipitates that precipitate have been identified as cementite (Fe_3C) [Ref. 31:p. 638]. Though the presence of Fe_3C has been reported by many authors, it should be noted that Speich did not find these precipitates in a low carbon martensitic steel due to the small thickness of his sample. The carbide precipitates did not have sufficient time to form during quenching [Ref. 33:p. 2554]. Depending upon the carbon content of the steel, these carbides may not be able to be imaged in the TEM and the use of x-ray diffraction may be required. [Ref. 34:p. 80]

In the high copper HSLA-100 steel, the high martensite start temperature (~450°C) and low carbon content will allow auto-tempering to take place. As it is quenched, the steel should go through the autotempering stage when small Fe_3C precipitates are formed. During tempering, the first stage is omitted and the third stage consists solely of the precipitation of Fe_3C. The tempering mechanism was reported by Chilton and Kelly and Speich [Ref. 31] [Ref. 33]

Lement, Averbach, and Cohen, report that the highest temperature at which the epsilon carbide is present is a temperature range of 243°C to 316°C. The temperature range for

the present of Fe_3C is reported to be 248°C to 499°C [Ref. 35:p. 869]. This data shows that the carbide expected to precipitate in the as-quenched microstructure should be Fe_3C since the auto-tempering process should be complete by about 350°C. [Ref. 31:p. 638].

Tempering at ~500°C results in the presence of tempered Fe_3C [Ref. 29:p. 11]. When tempering at temperatures of about 700°C and above, alloy carbides, eg., Cr_7C_3, will be the dominant precipitate. [Ref. 29:p. 11]

The temperature ranges for the stages of tempering as reported by Krauss are as follows: [Ref. 27:pp. 200-201]

Stage I: 100 to 250°C

Stage II: 200 to 300°C

Stage III: 250 to 350°C

Though there are temperature overlaps, these temperatures are generally accepted for the beginning of the first, second and third stages of tempering. [Ref. 37:pp. 202-204]

These overlaps in the temperature ranges of the stages of tempering account for the variation of results presented by Seal and Honeycomb, Chilton and Kelly, Aborn, Payson, Speich, Lement, Averbach and Cohen, and Hirotsu and Nagakura [Refs. 29, 31, 32, 33, 34, 35, 36, 38, 39]. Seal and Honeycomb, Chilton and Kelly, Aborn, and Payson show evidence of Fe_3C. However, Speich, Lement, Averbach and Cohen, and Hirotsu and Nagakura show evidence of either the η-carbide or the ε-carbide. The different tempering temperatures used, the

tempering times, the amount of carbon present in the steel, and the type of quench may account for the variation in the results.

D. SCOPE OF PRESENT WORK

The replacement of the HY series of steels used in ship construction is being actively pursued by the U.S. Navy and David Taylor Research Center. The HSLA series of steels is being investigated and certified to replace the HY series. HSLA-80 and HSLA-100 have been certified to replace their HY counterparts. A preliminary investigation has begun and is looking into using high copper HSLA-100 as the replacement for HY-130.

Previous work on the HSLA series has been concerned with the verification of mechanical and welding properties, examination of the microstructure at various aging temperatures, and changing the content of the alloying elements. It is generally agreed that the HSLA series of steels has a microstructure comprised of small packets of either bainitic ferrite or lath martensite with small amounts of retained interlath austenite in the as-quenched condition. The strength and toughness of these steels is attributed to the fine grained martensitic/bainitic microstructure, high dislocation density, and the aging characteristics of copper.

In this work, the effect of increased copper on the HSLA-100 steel will be examined to see if it meets the 130 ksi

yield strength criterion. Data will be collected on the microhardness, mechanical properties and the microstructural changes compared to the HSLA-100 steel. Transmission Electron Microscopy will be utilized to examine the effect of the aging behavior of copper on the microstructure of HSLA-100 steel.

III. EXPERIMENTAL PROCEDURE

A. MATERIAL

Five heat treated high copper HSLA-100 plate steel Charpy halves were provided by David Taylor Research Center (DTRC), Annapolis, Maryland, for this study. These samples (DTRC code GLB) were processed from the same cast by the Phoenix Steel Company and the exact processing information was reported previously by Mohr [Ref. 2:p. 31]. Of the five samples, one was in the as-quenched form and the others were aged for one hour at the following temperatures: 538, 566, 593, and 621°C. The Charpy halves were from a plate with a thickness of 19.05 mm and the samples were cut from these plates along the T-L orientation. Table III shows the chemical composition of the samples as defined by DTRC [Ref. 40:p. 14]

B. MECHANICAL PROPERTIES

Data for Charpy V-notch Impact Energy, ultimate tensile strength, 0.2% yield strength, percent reduction in area, and percent elongation were provided by DTRC [Ref. 40:p. 15]. The test data for strength and ductility are listed in Table IV and the Charpy test data is listed in Appendix A.

TABLE III. HIGH COPPER HSLA-100 STEEL LOT GLB COMPOSITION

Element	Actual Composition
C	0.047
Mn	0.85
P	0.010
S	0.005
Si	0.22
Ni	3.59
Cr	0.57
Mo	0.60
Cu	2.00
Cb	0.025

TABLE IV. DTRC TENSILE TEST RESULTS FOR HIGH COPPER HSLA-100, DTRC CODE GLB

Aging Temperature (°C)	0.2% Yield Strength (KSI)	Ultimate Strength (KSI)	Percent Elongation	% Reduction in Area	YS/UTS
As Quenched	133.5	162	16.5	65	0.825
538	148	152	17.5	66	0.97
566	147	147.5	18	67.5	0.995
593	138.5	139	20	70	0.995
621	130	130	20.5	73	1.0

C. MICROSCOPY

1. Optical Microscopy

Optical Microscopy was conducted to photograph and analyze the etched microstructure. An inclusion study has been previously completed by Mohr [Ref. 2:pp. 39-48] for the as-quenched sample.

All samples were mounted in non-conducting bakelite. After mounting, the samples were ground on a rough grit grinder to ensure a smooth surface for subsequent polishing. The samples were then polished using 240 grit, 320 grit, 400 grit, and 600 grit sandpaper. Upon completion of polishing by sandpaper, the samples were washed with soap and water, followed by a cleaning with ethanol and blown dry.

The samples were then polished on a six micron polishing wheel using diamond paste. After satisfactory polishing on the six micron polishing wheel, the samples were then washed using soap and water and finally a cleaning with ethanol and blown dry prior to polishing on the one micron polishing wheel. After polishing on the one micron polishing wheel with diamond paste, the samples were cleaned with soap and water again and cleaned with ethanol and blown dry. The samples were then etched with a two percent nital solution for approximately 45 seconds.

The samples were then placed in a Zeiss ICM 405 photomicroscope and were examined at various magnifications. Photomicrographs were taken at 200X and 1000X as these seemed to provide the most information.

2. Scanning Electron Microscopy

After optical examination, the samples were then placed in a Cambridge Stereo Scan S200 Scanning Electron Microscope and examined. Micrographs were then taken at

approximately 500X and 1500X as these magnifications provided the best information. Micrographs were taken using secondary electron images and back-scattered electron images. From this, martensite packet sizes of the as-quenched sample were determined to be in agreement with earlier work by Mohr [Ref. 2:pp. 58-59].

3. Transmission Electron Microscopy

Thin wafers were cut from the as-quenched peak-aged (538°C), and over-aged (621°C) Charpy samples using a low speed diamond wafer saw. Three various orientation (0°, 45°, and 90°) were cut from each sample so that various crystallographic zone axes could be observed. This would prove to be important to enable photography of the various crystallographic zone axes and orientations.

After cutting the thin wafers of approximately 0.25 mm in thickness, the samples were then thinned using wet 200 grit sandpaper to approximately 0.18 mm. Then, 320 grit wet sandpaper was used to thin the samples to approximately 0.11 mm. The samples were then punched out to 3 mm diameter discs. Using 400 grit wet sandpaper, the samples were then thinned to approximately 0.05 mm thickness. After an ethanol bath, the samples were then thinned to approximately 0.02 mm thickness using wet 600 grit sandpaper.

Upon completion of thinning, the samples were electrochemically thinned to perforation in a Struers Tenupol

electropolishing device operating at 70 volts and 0.5 amperes. A solution of 3% perchloric acid, 62% ethanol, and 35% n-butoxy ethanol solution cooled to approximately - 20°C was utilized with a setting of three on the Tenupol device.

After electropolishing, a Gatan Dual Ion Mill (Model 600) Machine was utilized to remove redeposited copper on the samples. The ion mill machine was operated at room temperature using two guns at a current of 0.5 amperes and a voltage of 5.0 kilovolts for 30 minutes at an angle of 15 degrees.

Redeposited copper is a problem with the high copper HSLA-100 samples as evidenced by incorrect results reported by Mohr [Ref. 2:pp. 63-66]. These erroneous conclusions can be avoided by increasing the milling times to 30 minutes or longer. Figures 6 and 7 show the "incorrect" results using only 10 minutes of milling time as previously reported by Mohr [Ref. 2:p. 35]. These micrographs show the presence of "ε copper precipitates" in the microstructure of high copper HSLA-100 steel in the as-quenched condition.

Upon completion of electropolishing and ion milling, the samples were placed in a JEOL Model JEM 100 CX transmission electron microscope operated at 120 KV and examined. Composition of second phase particles - e.g. carbides were determined using a Kevex energy dispersive X-ray analyzer. The martensitic lath widths were measured and were in agreement with earlier data supplied by Mohr [Ref. 2:p. 59].

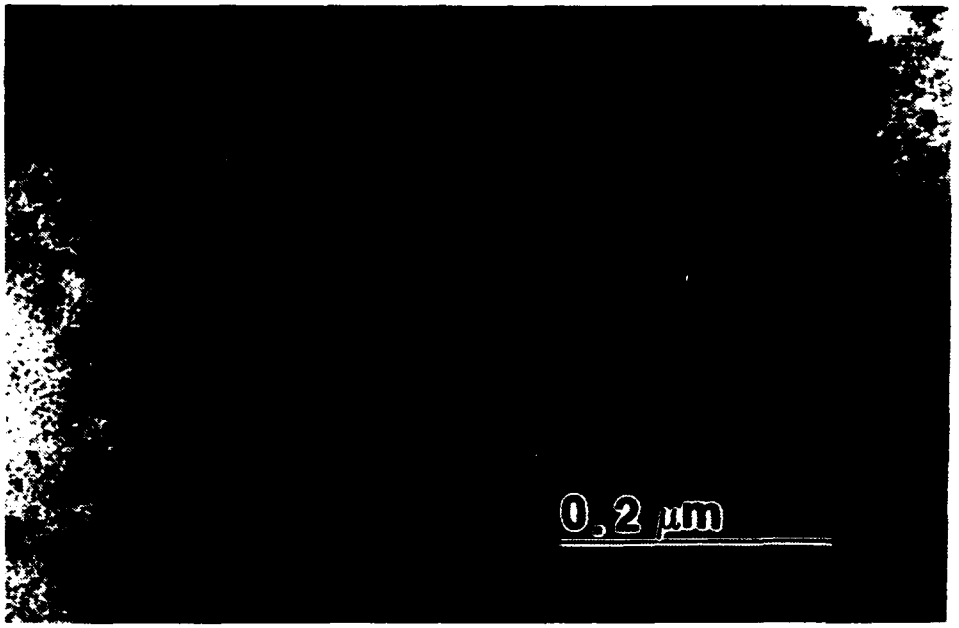

Figure 6 TEM Image Showing the Presence of ε Copper Precipitates in the Microstructure of High Copper HSLA-100 Steel.

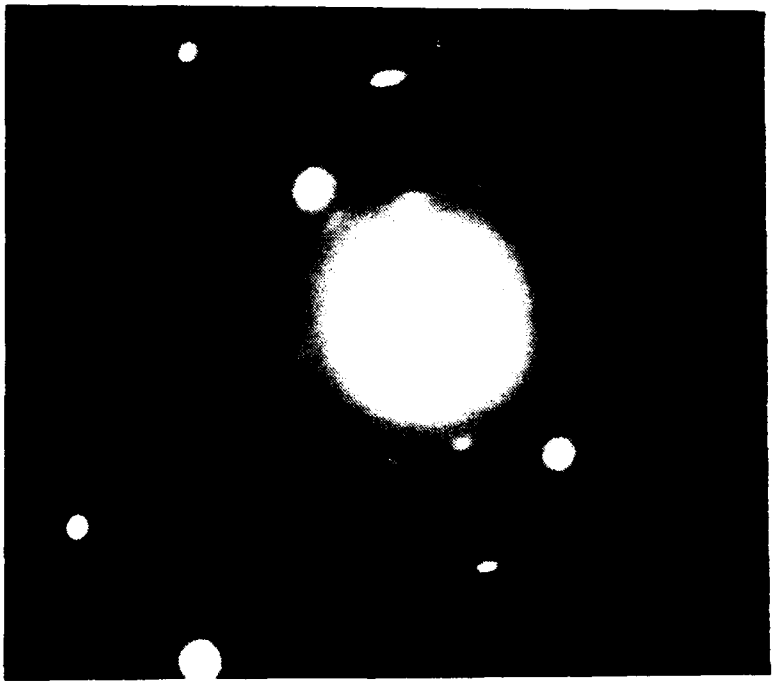

Figure 7 Selected Area Diffraction Pattern (SADP) Showing Presence of ε Copper Precipitates.

D. MICROHARDNESS TESTING

A microhardness test was conducted on the as-quenched 19.05 mm plate sample provided by DTRC. A Micromet Microhardness Tester was utilized to conduct the microhardness test. The microhardness test was done to determine the decrease in hardness versus the distance from the outer surfaces.

Preparation of the sample was performed in the same manner as preparation for optical microscopy with the exception of etching the sample. The sample was then placed in the Micromet Microhardness Tester and weights of 100, 200 and 300 grams were used to determine the Vickers Hardness Number at intervals of 0.05 mm starting at each edge and working toward the center of the plate. The sample was tested three times with each weight for repeatability and average values were used to determine the microhardness.

IV. RESULTS AND DISCUSSION

A. MECHANICAL BEHAVIOR

Variations of high copper HSLA-100's yield strength and toughness are shown in Figure 8. The relationship between ultimate tensile strength and 0.2% yield strength versus aging temperature is shown in Figure 9. The yield strength peaks at 538°C and then decreases at the higher aging temperatures. The ultimate tensile strength peaks in the as-quenched condition and also decreases as the steel is aged. At 621°C, the yield strength has actually fallen to the 130 ksi yield strength, but still meets the criteria. The strength behavior exhibited is characteristic of the aging behavior associated with copper precipitation upon aging [Ref. 7:p. 50]. Figure 10 shows toughness values measured by conducting Charpy V-Notch (CVN) impact tests on specimens cooled to -84°C. This shows the toughness decreasing until a minimum is reached at the peak aged temperature of 538°C and at the same time, the yield strength is at the maximum. Upon overaging, the toughness of the steel rises dramatically. At the 621°C aging temperature, the CVN energy is more than twice as high as the values obtained for 538°C. Figure 10 shows the ductile to brittle transition temperature (DBTT) behavior of the high copper HSLA-100 steel at the various aging temperatures. It can be

seen that the impact energy decreases to a minimum at the 538°C aging temperature and at 621°C, the values are approximately twice as great. The DBTT curves of the as-quenched and 566°C are very close to identical.

In order to measure the ductility of the steel, percent reduction in area and percent elongation are two parameters used to determine the ductility of the steel. Figure 11 shows these characteristics as a function of aging temperature. The percent elongation measurement remains fairly constant during aging. The percent reduction of area measurement was seen to increase slightly upon aging. The above mechanical testing results on lot GLB exceed the strength and toughness requirements for HY-130 steel listed in Table V. Lot GLB also exceeds the percent elongation and reduction in area requirements for HSLA-100 steel listed in Table VI.

TABLE V. HY-130 STEEL STRENGTH AND TOUGHNESS REQUIREMENTS

0.2% Yield Strength	896 MPa minimum
Transverse Charpy V-Notch Impact Toughness	81.3J at -19°C 54.2J at -84°C
Percent Elongation	15% minimum in 50.8 mm

TABLE VI. HSLA-100 DUCTILITY REQUIREMENTS

Percent Elongation Percent Reduction in Area	18% minimum in 50.8 mm 45% minimum

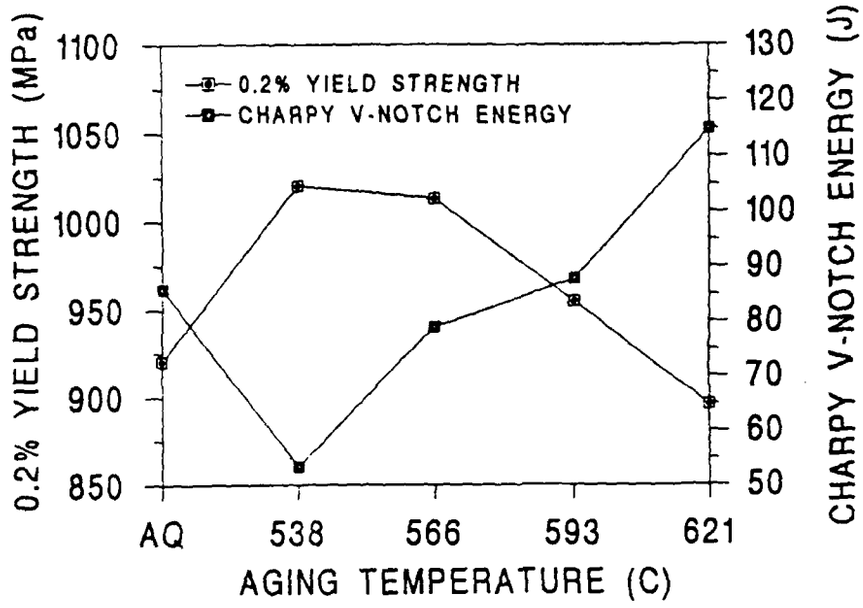

Figure 8 High Copper-HSLA-100 Steel Lot GLB 0.2% Yield Strength and Impact Energy at -84°C as a Function of Aging Temperature

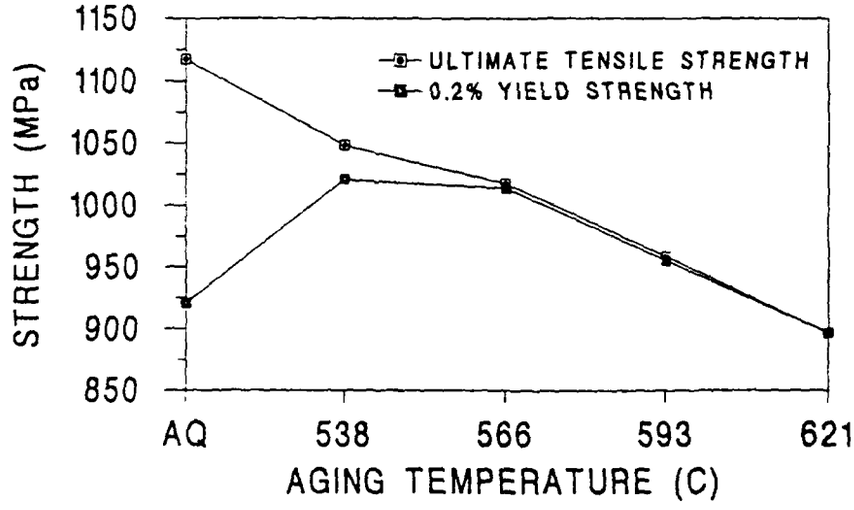

..gure 9 High Copper HSLA-100 Steel Lot GLB 0.2% Yield Strength and Ultimate Tensile Strength

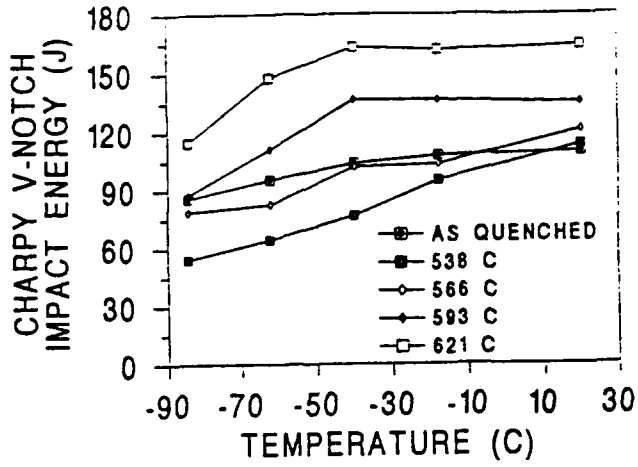

Figure 10 High Copper HSLA-100 Steel Lot GLB DBTT Behavior at Various Aging Temperatures

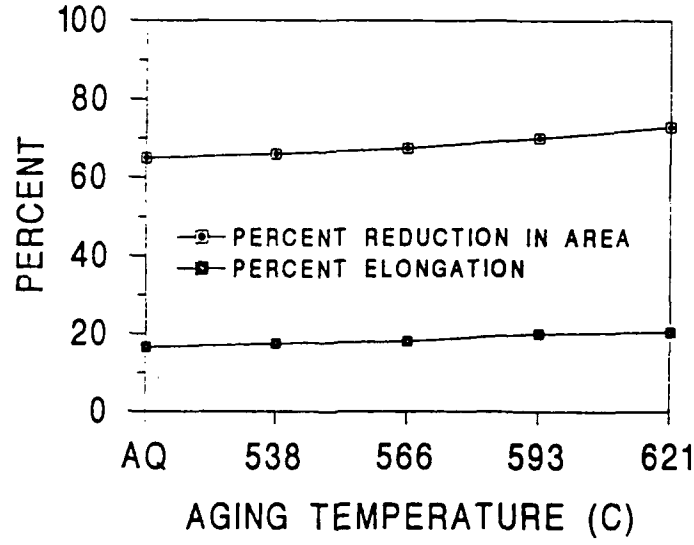

Figure 11 High Copper HSLA-100 Steel Lot GLB Ductility: Variation of Elongation and Reduction of Area with Aging Temperature

The mechanical property data provided by DTRC shows the best combination of strength and toughness occurs at the peak aging condition of 538°C; the microstructure of this optimum specimen will be examined in the present work. The overaged condition (621°C) will be examined due to its high toughness. The as-quenched, initially examined by Mohr, will also be reassessed.

B. MICROHARDNESS

A microhardness test was performed on an as-quenched 19.05 mm plate sample provided by DTRC. Results are shown in Figure 12.

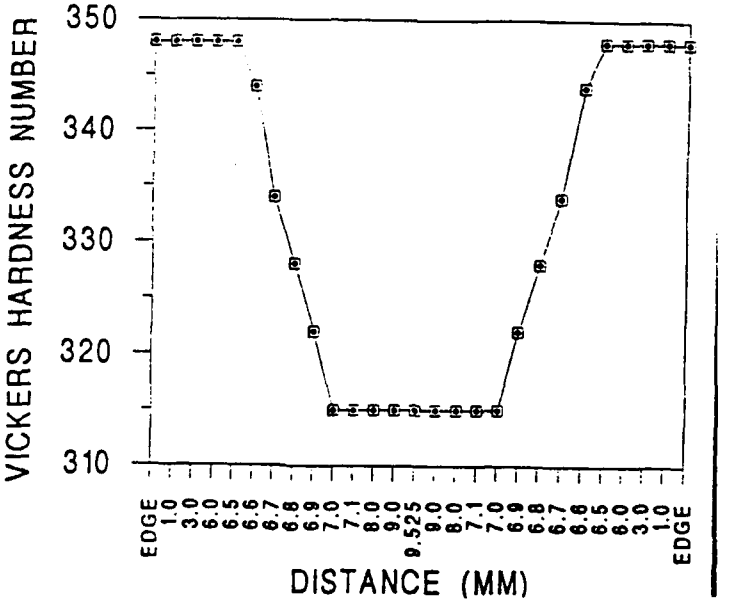

Figure 12 **Vickers Hardness Number Versus Distance from the Center of the As-quenched High Copper HSLA-100 19.05 mm Plate**

The results obtained from the microhardness test seem to verify the martensitic microstructure. The middle of the plate probably contains some bainitic ferrite mixed with the lath martensite. The results obtained seem to be in agreement with earlier data on microhardness reported by Speich [Ref. 35:p. 2558]. Figure 13 shows that the hardness results are in agreement with previous work.

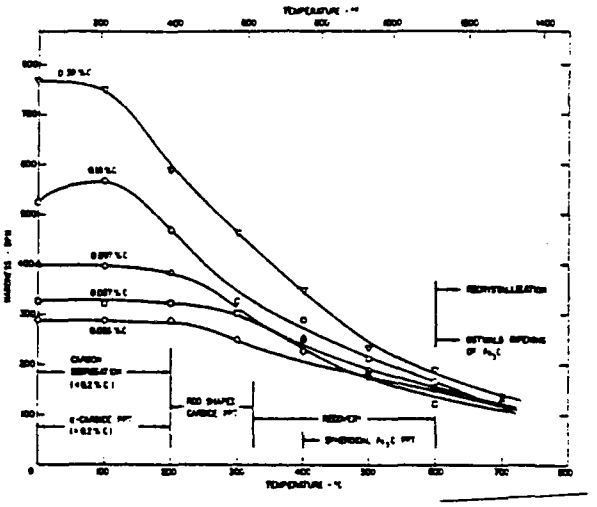

Figure 13 Hardness Results for Various Iron Carbon Martensites [Ref. 33:p. 2558]

C. MICROSTRUCTURE

All samples received of lot GLB were examined using optical and scanning electron microscopy. The as-quenched, 538°C, and 621°C were examined using transmission electron

microscopy. The microstructures of each were characterized and correlated to their mechanical properties.

1. As-Quenched High Copper HSLA-100 Steel

Figure 14 shows an optical micrograph of the as-quenched high copper HSLA-100. In this micrograph, the transformation product packet size was determined in conjunction with Figure 15. The transformation product packet is lath martensite and a small amount of retained austenite as thin films at lath boundaries (approximate size of 200-300 Å). The amount of retained austenite should be less than one percent of the total transformation product packet [Ref. 30:p. 724]. Sarikaya, *et. al.* report that for a 0.15 weight percent carbon steel, the retained austenite contains approximately 0.9 weight percent carbon [Ref. 41:p. 1424]. Since high copper HSLA-100 steel is approximately 0.05 weight percent carbon, the carbon content of retained austenite expected to be 0.3 or 0.4 weight percent carbon. From an examination of the HSLA-100 steel CCT diagram (Figure 2), this microstructure is expected. This sample was obviously taken from the order edge of the 19.05 mm plate due to the absence of bainitic ferrite. This is in agreement with the microhardness data in the previous section.

Figures 16 and 17 are TEM micrographs showing the general microstructure of lath martensite. Figure 18 and 19 are TEM micrographs showing autotemper Fe_3C carbides and the

high dislocation density. These were expected for this low carbon, high martensite start temperature steel. Retained austenite is observed in the bright field micrograph of Figure 20. In the dark field micrograph of Figure 21, the retained austenite is illuminated. Copper precipitates were not evident as previously reported by Mohr [Ref. 2:p. 35] and this can be seen by Figures 22, 23 and 24. There is no evidence of streaking as the selected area diffraction patterns (SADP) show. It had been reported by Howell that copper precipitates can be present on quenching, but the specimens he used were oil-quenched, allowing a slower cooling rate [Ref. 42:p 902].

The transformation product packet size, consisting of martensite and possibly bainitic ferrite was found to be less than 7μm. Fine austenite grain size leading to a small transformation product packet size and the highly dislocated martensite microstructure seem to be the main strengthening mechanisms. Molybdenum, copper, chromium and nickel provide solid solution strengthening. Toughness can be attributed to the small transformation product packet size and the fine martensitic laths which will deflect dislocations and cracks.

2. 538°C Aged High Copper HSLA-100 Steel

An optical micrograph is shown in Figure 25 and a SEM micrograph is shown in Figure 26. These figures show the slightly larger transformation product packet size. These packets are composed of tempered lath martensite and are

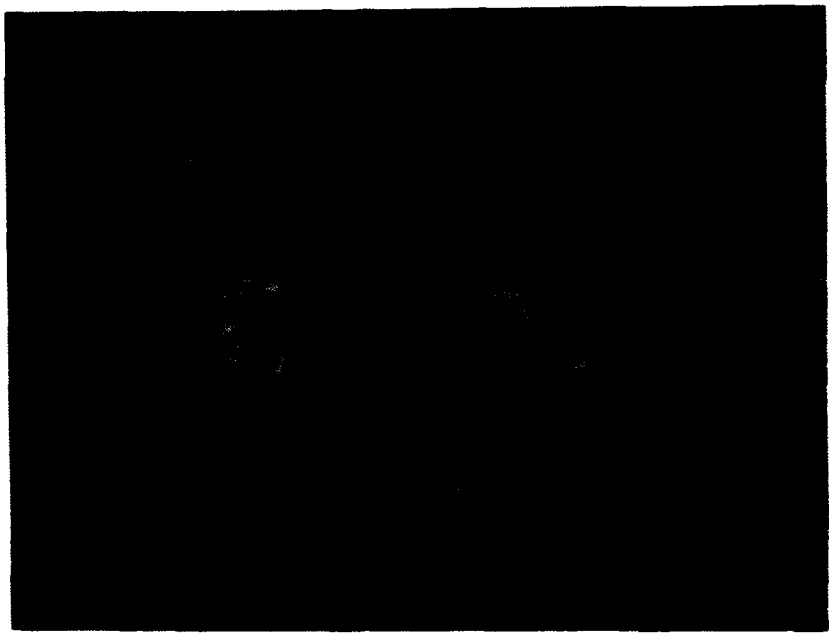

Figure 14 Optical Micrograph of As-Quenched Transformation Product Packets

Figure 15 SEM Micrograph of As-Quenched Transformation Product Packets

Figure 16 TEM Image Showing Lath Martensite and Retained Austenite at Lath Boundaries

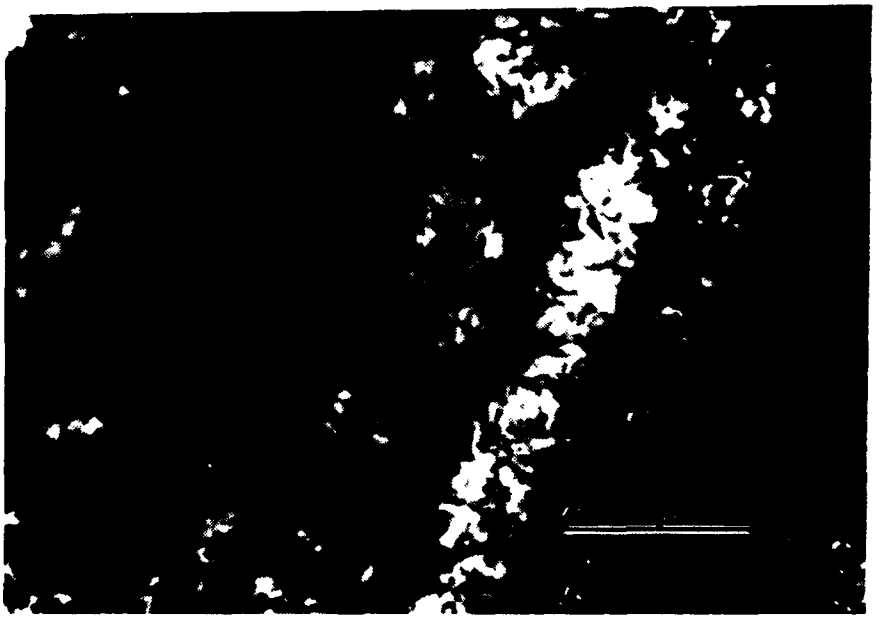

Figure 17 TEM Image Showing Lath Martensite and Retained Austenite at Lath Boundaries

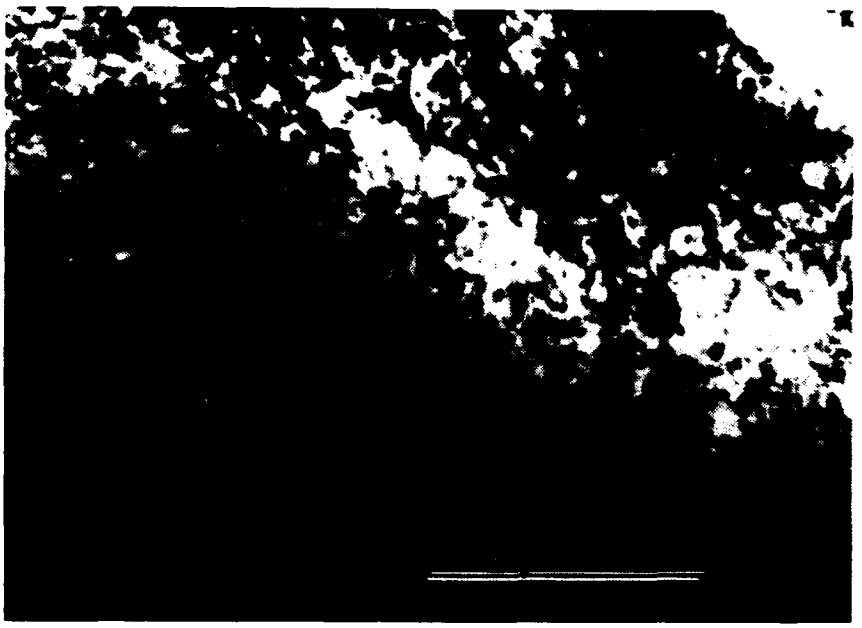

Figure 18 TEM Image Showing Carbide Precipitates

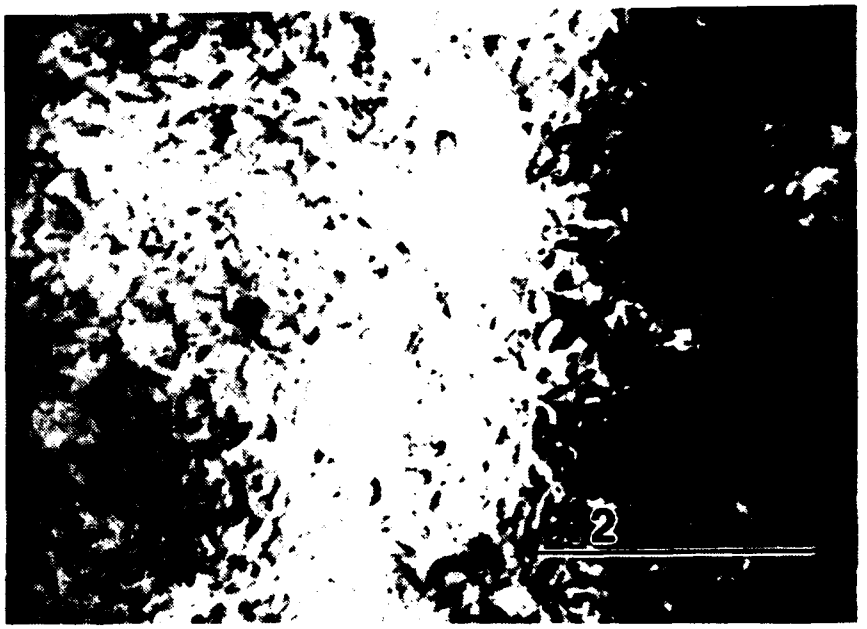

Figure 19 TEM Image Showing Carbide Precipitates

Figure 20 TEM Bright Field Image Showing Retained Austenite at Lath Boundaries

Figure 21 TEM Dark Field Image Showing Retained Austenite at Lath Boundaries

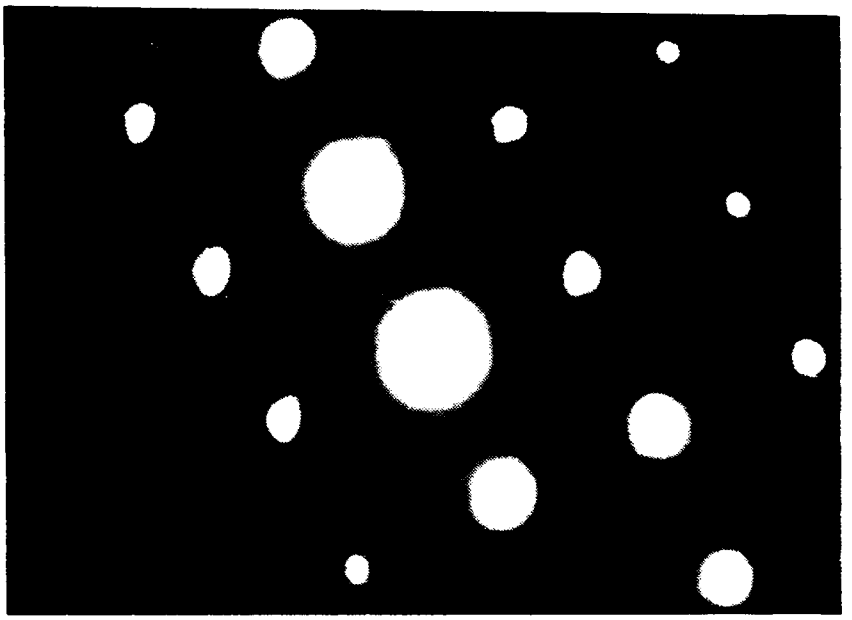

Figure 22 Diffraction Pattern Showing a [001] Crystallographic Zone Axis (Note the Faint Spots Attributed to Fe_3C Precipitates)

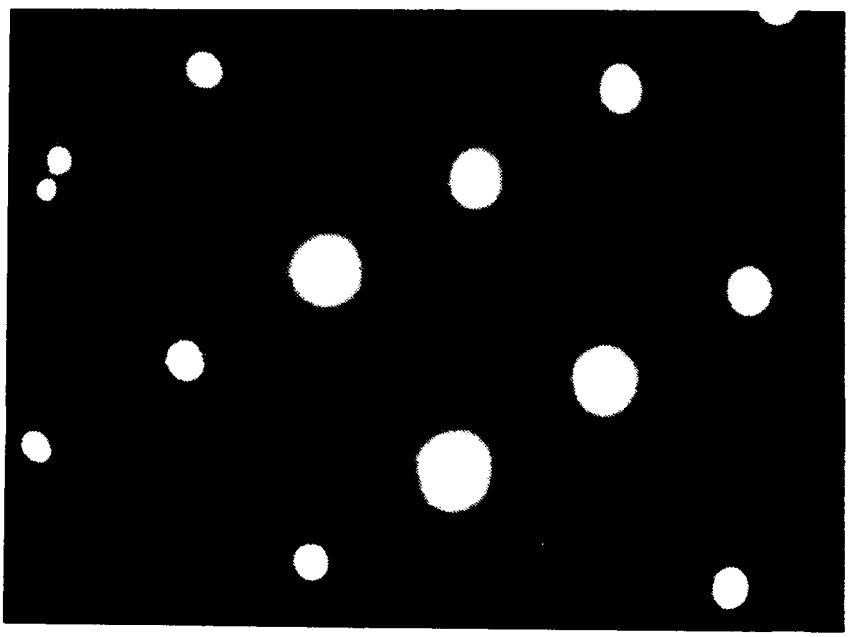

Figure 23 Diffraction Pattern Showing a [011] Crystallographic Zone Axis. (Note the Faint Spots Attributed to Fe_3C Precipitates)

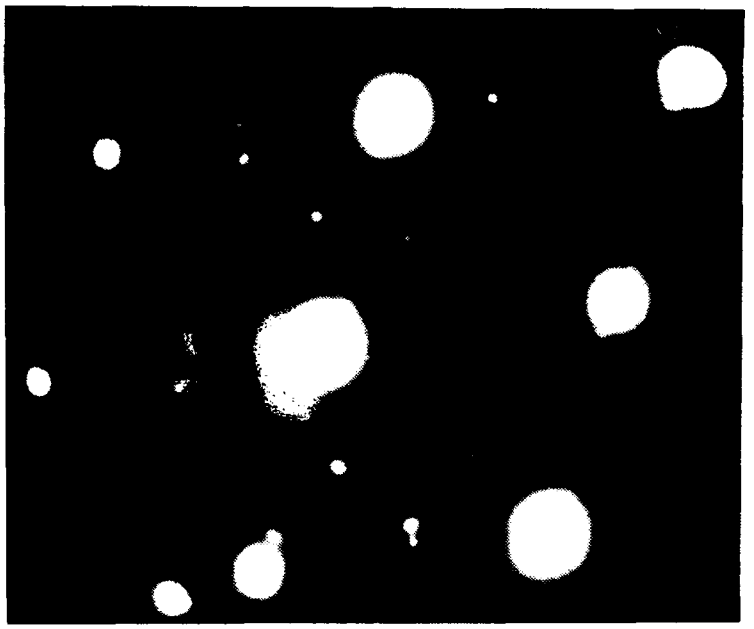

Figure 24 Diffraction Pattern Showing a [012] Crystallographic Zone Axis. (Note the Faint Spots Attributed to Fe_3C Precipitates)

slightly larger than 7 μm. Coherent BCC copper precipitates are present but are not visible due to their small size. Figures 27 and 28 show the general microstructure of the tempered lath martensite. Tempered Fe_3C precipitates are seen decorating dislocations in Figure 29 and 30. These carbide precipitates are larger than those present in the as-quenched condition. Figure 31 shows the coherency strain fields associated with the BCC copper precipitates. The coherent copper precipitates were not able to be successfully imaged in the TEM due to their small size (~ 12-20 Å) but could be seen in the SADP. Figures 32 and 33 show SADPs at two different crystallographic zone axes. These figures suggest that the

carbides are a result of tempering and are perhaps beginning to transform to $(FeM)_3C$ carbides present in the overaged condition. Figure 34 shows a selected area diffraction pattern showing evidence of the coherent BCC copper precipitates.

Peak strength is achieved in this specimen. Significant additional strengthening is provided by copper age hardening. Previous work suggests that the size of the copper precipitates are on the order of 20 Å [Ref. 24]. The coherency strain fields associated with the BCC copper precipitates also contribute to the increased strength. The coherency strain fields block dislocations thus higher stress is required for dislocation motion. The larger carbide precipitates and dislocation substructures also contributed to the increased strength.

Since dislocation motion is impeded, the toughness goes to a minimum at this aging temperature. This mechanical behavior is typical of peak aged coherent precipitate hardened copper bearing steels. [Ref. 7:p. 59]

3. 621°C Aged High Copper HSLA-100 Steel

Figures 35 and 36 show the overaged microstructure of high copper HSLA-100 steel. The transformation product packet size is approximately 10 μm and the lath width has widened considerably from the as-quenched condition. This increased lath width can be seen in Figure 37. Incoherent ε-copper precipitates are now visible having replaced the coherent BCC

Figure 25 Optical Micrograph of 538°C Aged Transformation Product Packets

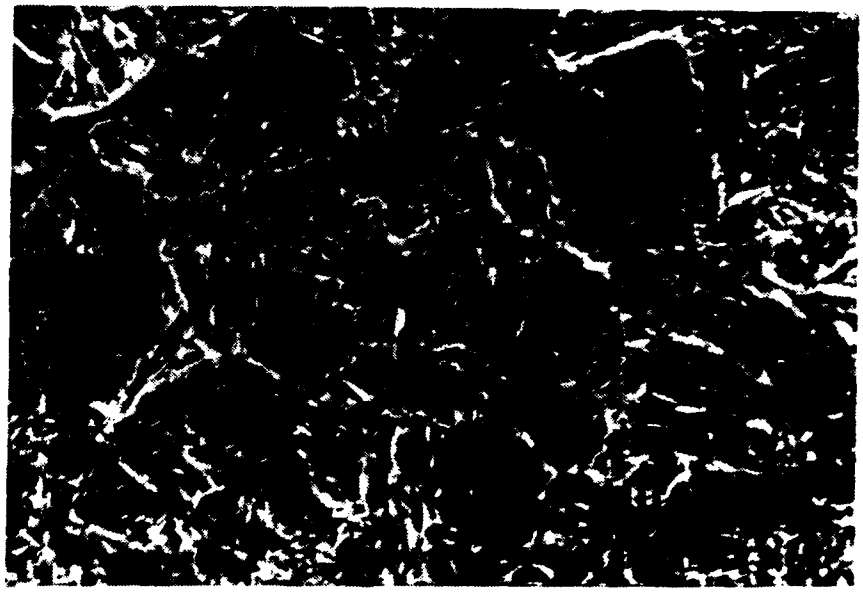

Figure 26 SEM Micrograph of 538°C Aged Transformation Product Packets

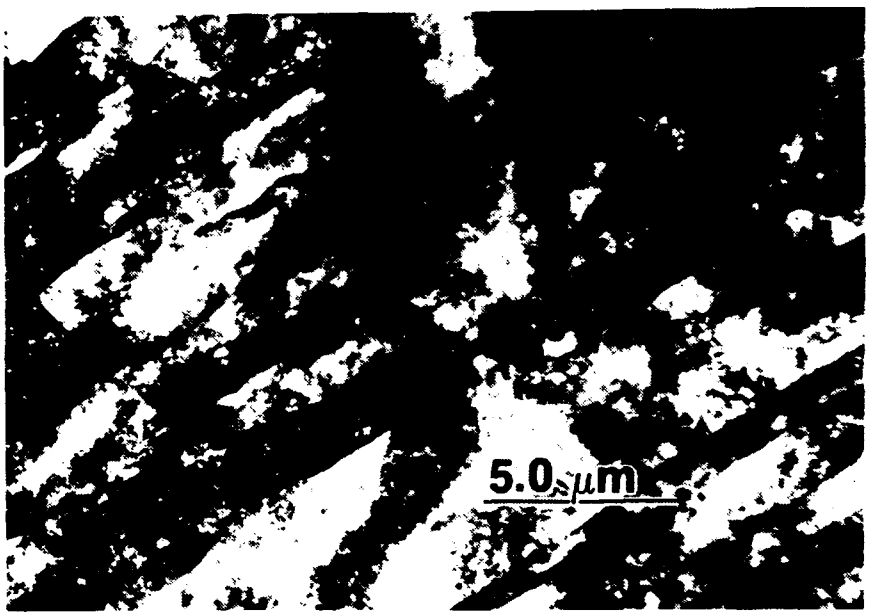

Figure 27 TEM Image Showing Tempered Lath Martensite Microstructure

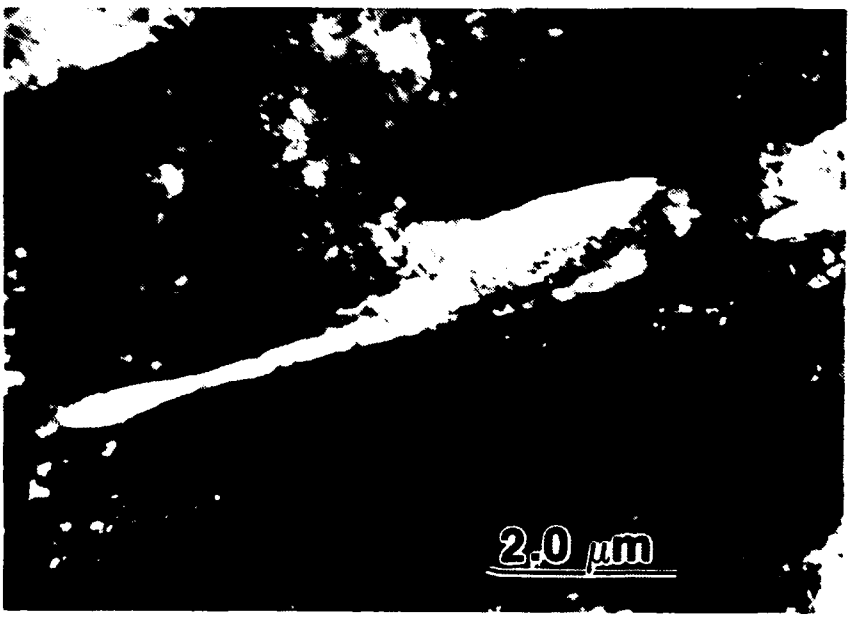

Figure 28 TEM Image Showing Tempered Lath Martensite Microstructure

Figure 29 TEM Image Showing Tempered Fe_3C Precipitates Decorating Dislocations

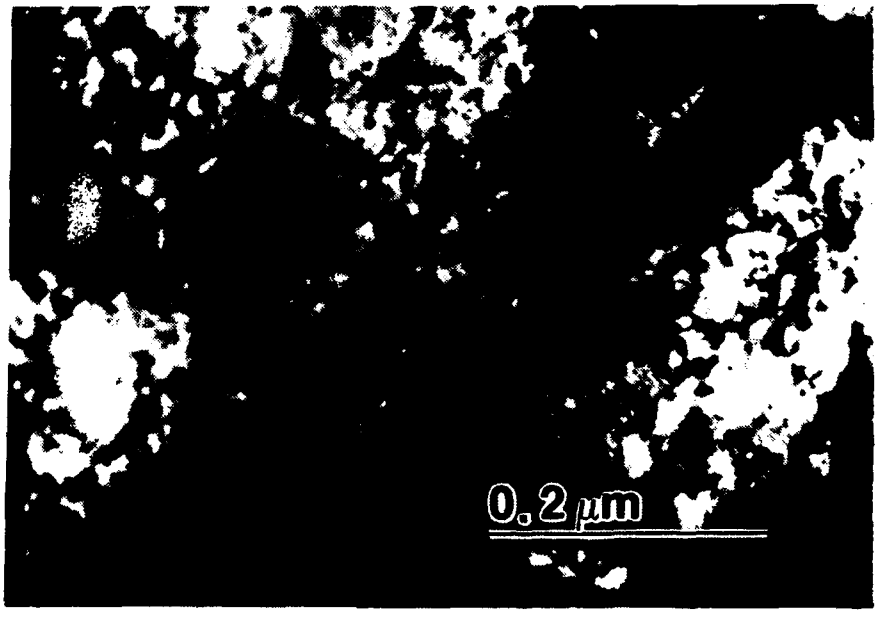

Figure 30 TEM Image Showing Tempered $(FeM)_3C$ Precipitates Decorating Dislocations

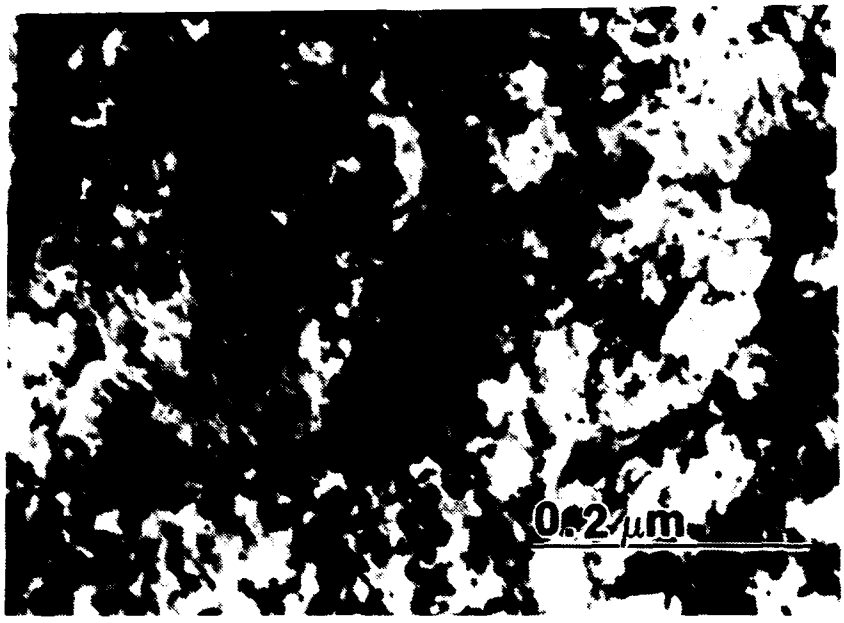

Figure 31 TEM Image Showing Coherent BCC Copper Precipitate Coherency Strain Fields

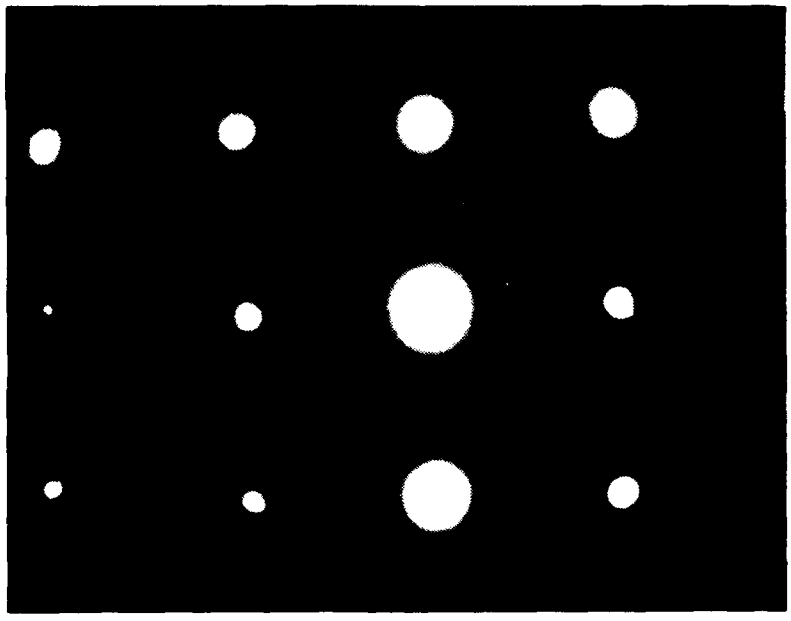

Figure 32 Diffraction Pattern Showing a [001] Crystallographic Zone Axis. (Note That There Are Less Faint Spots Due to the Fe_3C Precipitates)

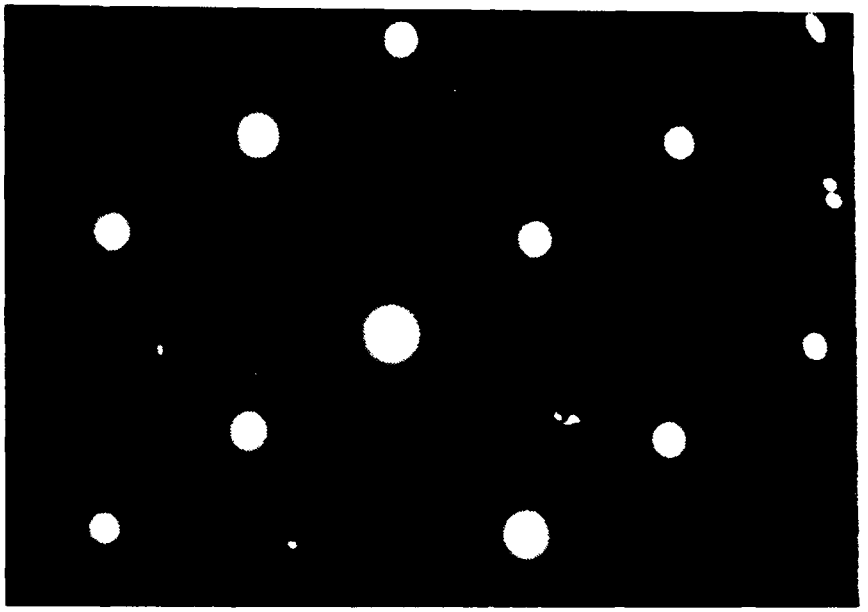

Figure 33 Diffraction Pattern Showing a [011] Crystallographic Zone Axis. (Note That There Are Less Faint Spots Due to the Fe_3C Precipitates)

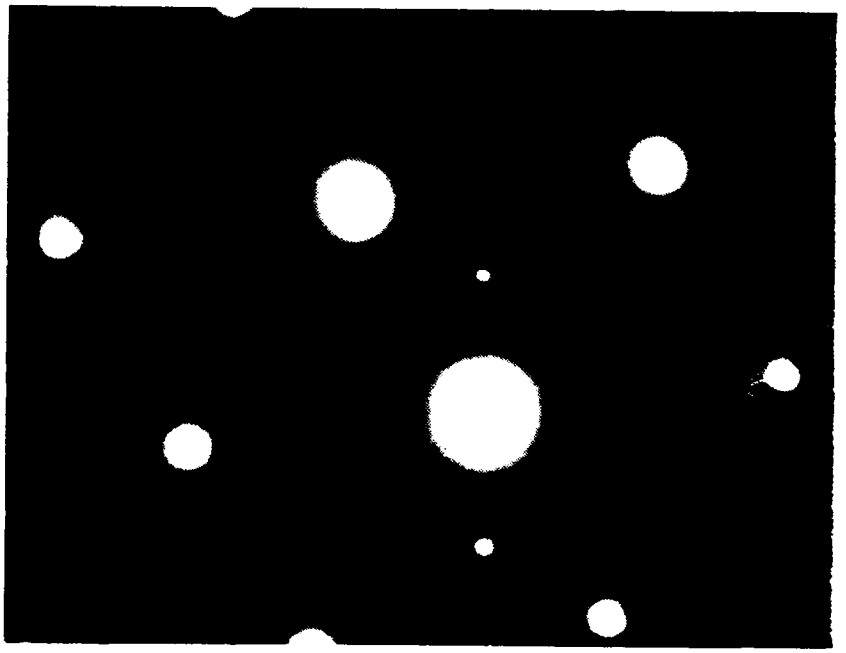

Figure 34 Diffraction Pattern Showing a [012] Crystallographic Zone Axis. (Note That There Are Less Faint Spots Due to the Fe_3C Precipitates)

type precipitate. These copper precipitates can be seen decorating dislocations and lath boundaries in Figure 38. Figure 39 also shows incoherent FCC precipitates. Figure 38 also shows a niobium carbide or carbonitride that has now precipitated in the overaged condition. These carbides are of the NbCN type and can be seen in Figures 40 and 41. The coherent FCC copper precipitates are also present in the SADP, Figure 41. This SADP is complex and contains patterns from temper carbides (most likely $(FeM)_3C$) and ε-copper precipitates.

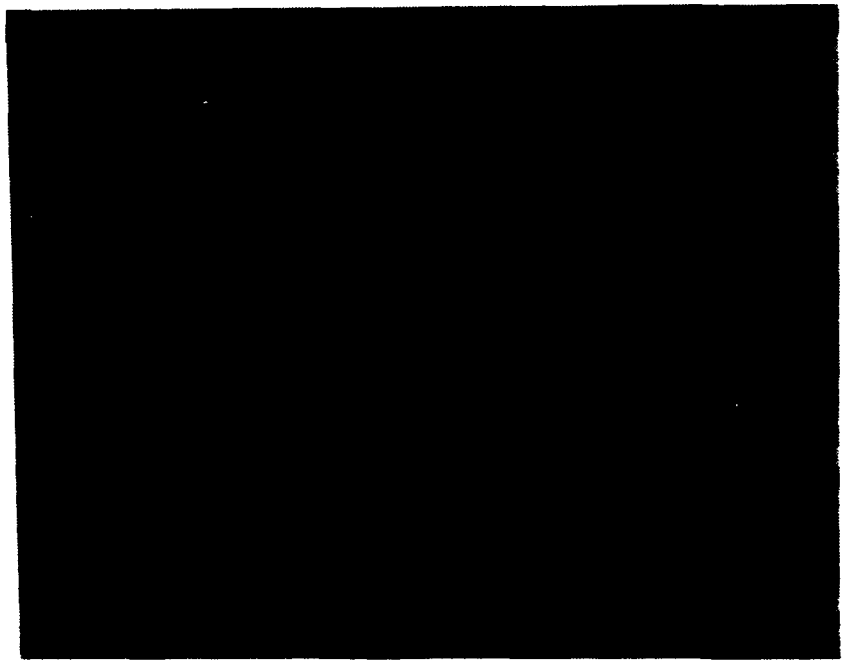

Figure 35 **Optical Micrograph of 621°C Aged High Copper HSLA-100 Steel Showing the Increased Transformtion Product Packet Size**

Figure 36 SEM Micrograph of 621°C Aged High Copper HSLA-100 Steel Showing the Increased Transformation Product Packet Size

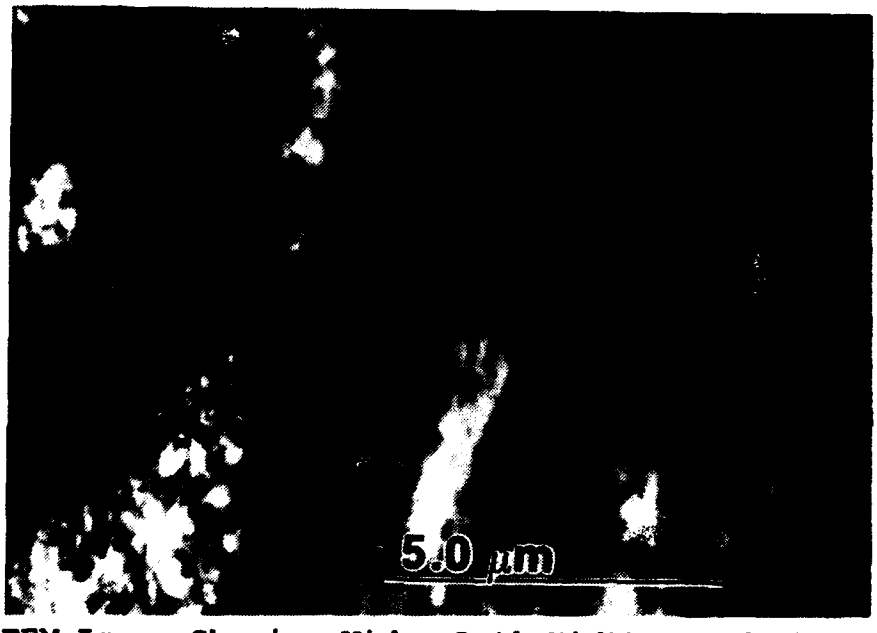

Figure 37 TEM Image Showing Wider Lath Widths of 621°C Aged High Copper HSLA-100 Steel

Figure 38 TEM Image Showing Incoherent FCC Copper Precipitates Decorating Dislocations and a Large Niobium Carbide or Carbonitride (arrowed)

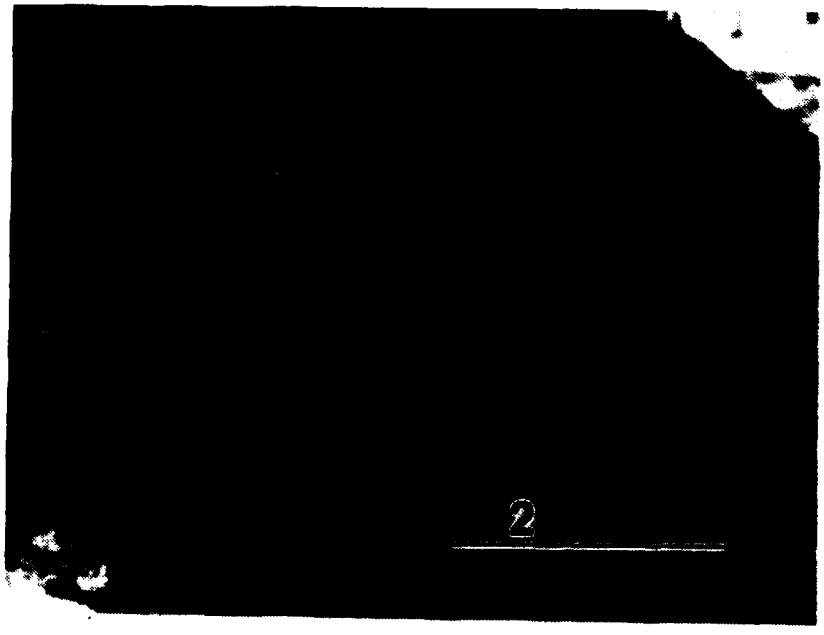

Figure 39 TEM Image Showing Incoherent FCC Copper Precipitates

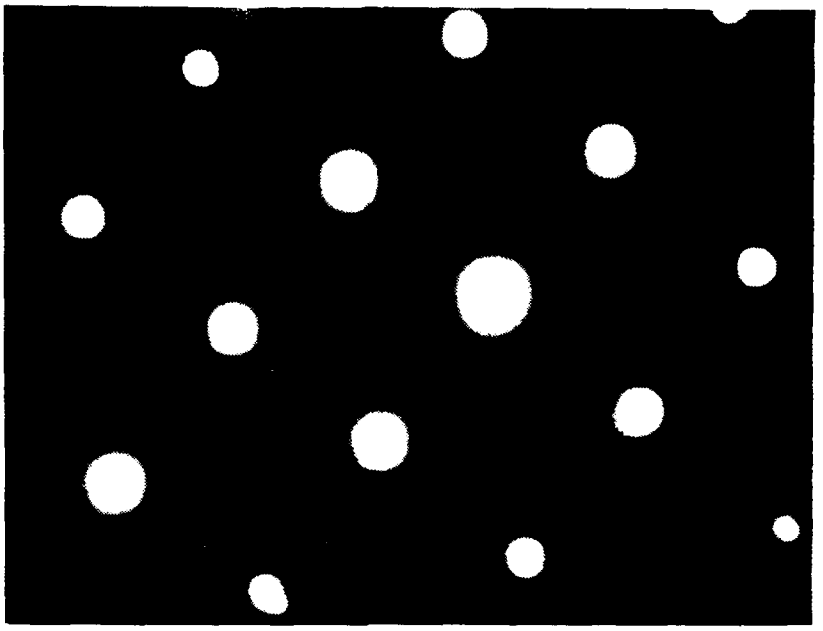

Figure 40 Diffraction Pattern of [001] Pole Showing Evidence of $(FeM)_3C$ Type Carbide

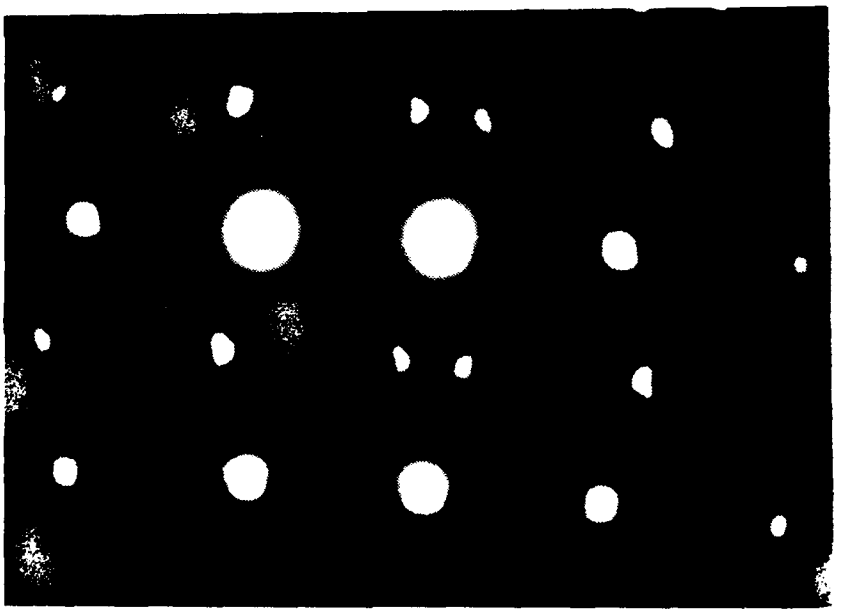

Figure 41 Diffraction Pattern of [011] Pole Showing Patterns of Incoherent FCC Copper Precipitates and $(FeM)_3C$ Type Carbides

The strength in the overaged condition is now at the 130 ksi minimum. The growth of the copper precipitates and their incoherence with the steel matrix is typical of age hardened materials. This will allow dislocations to move more freely, thus causing the reduction in strength. Recovery of the dislocation substructures causes the dislocations to have a smaller effect on strengthening. The tempered $(FeM)_3C$ carbides containing niobium and molybdenum tend to increase strength since they force dislocations to expend energy in bowing around the carbides and carbonitrides. This effect is reduced though since the dislocations are able to move more freely. Another detriment to the strength is the larger transformation product packet size.

Toughness is significantly increased, almost twice the value of the peak aged condition. The most significant contribution to this rise in toughness is probably due to the ductile overaged copper precipitates as they are apparently able to plastically deform and blunt propagating crack tips. Recovery allows dislocation motion to become easier and toughness will rise due to this effect. Finally, the intralath carbides contribute to the increase in toughness by acting as crack arrestors.

4. Transformation Product Packet Dimensions

Growth of transformation product packet size is shown in Figure 42. Figure 43 shows the increase in martensitic lath

width with aging. Transformation product packet size significantly increases beyond the peak aging (538°C) temperature. These results are consistent with the finding of Comerford and Mattes. [Ref. 7] [Ref. 18]

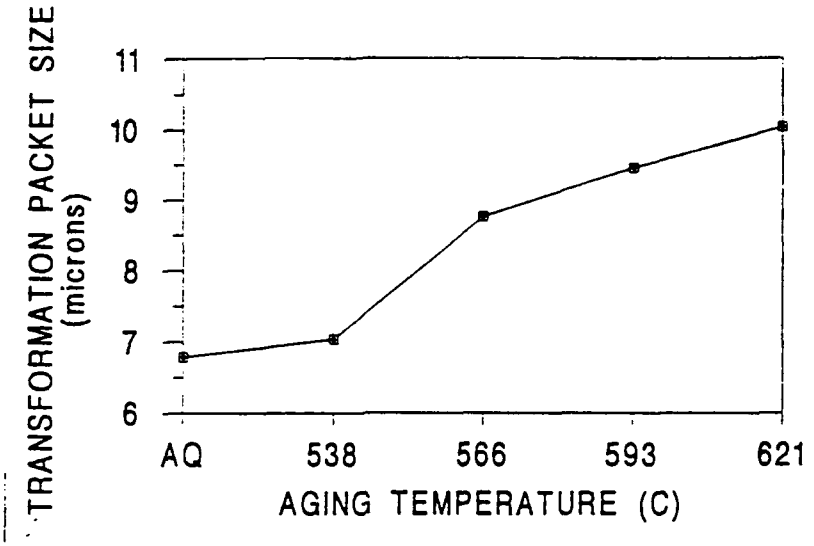

Figure 42 **Variation of Transformation Product Packet Size with Aging Temperature**

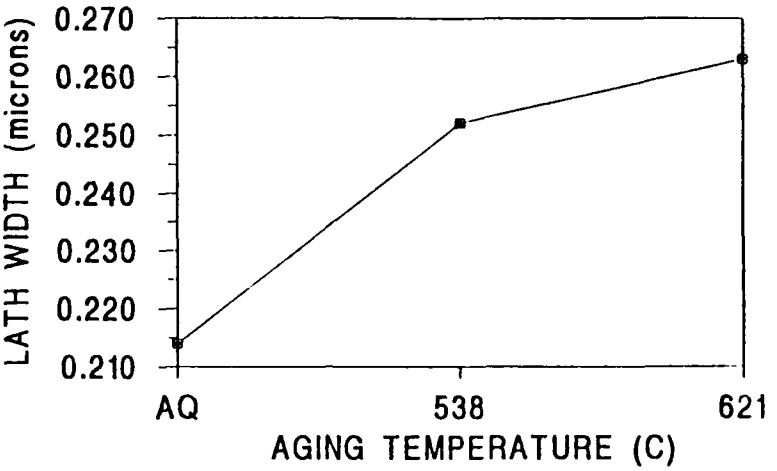

Figure 43 **Variation of Martensite Lath Widths with Aging Temperature**

V. SUMMARY

A. CONCLUSIONS

1. Mechanical Properties

All of lot GLB meets the minimum requirement for strength, toughness, and ductility. Of the five specimens provided by DTRC, the aging treatment at 538°C will give the best combination of strength, toughness, and ductility. The as-quenched sample could also be considered to give the best combination of mechanical properties.

2. Microhardness

The microhardness test showed that the samples provided by DTRC were not taken from the through thickness of the 19.05 mm plate. The microhardness tests verified the martensitic microstructure due to the minimal drop in Vickers hardness number. The decrease in microhardness suggests that the microstructure in the center of the plate may be bainitic ferrite rather then martensite.

3. Microstructure

Several complex microstructural mechanisms are responsible for high copper HSLA-100 steel's excellent strength and toughness. To correlate these mechanisms with the mechanical properties of the steel, the microstructure of the

as-quenched, peak aged (538°C) and overaged (621°C) specimens were studied in depth.

In the as-quenched condition, the main strengthening mechanisms present seem to be the small transformation product packet size and the highly dislocated martensitic microstructure. Also contributing to the impediment of dislocation motion is solid solution strengthening. Autotemper carbides also impede dislocation motion by forcing dislocations to bow around them. The toughness is influenced by the very fine martensitic laths and the small transformation product packet size which tend to deflect cracks and dislocations.

In the aged at 538°C specimen, peak strength is attained. This additional strengthening is due to the mechanisms involved in the as-quenched condition and the precipitation of small coherent BCC copper participates and the associated coherency strain fields which prevent dislocation motion. The tempered carbide precipitates present force dislocations to bow around them. At this aging temperature, the coherent BCC copper precipitates has an adverse effect on toughness which is now at a minimum. This treatment provides the best candidate as a replacement for HY-130 steel.

In the overaged condition (621°C), the strength still meets the 130 ksi yield strength criterion but the toughness is highly increased. The decrease in strength is due to the

development of incoherent FCC copper precipitates from the coherent BCC copper precipitates. Evidence of the recovery of the dislocation substructures can also be observed. Intralath carbides and carbonitrides and the ductility of the overaged copper precipitates markedly improve the toughness characteristics. Dislocation motion is also made easier and this contributes to the increase in toughness.

B. RECOMMENDATIONS

The U.S. Navy's pre-certification program for a suitable replacement for HY-130 is continuing and due to the problems encountered in the Seawolf class submarine, it should be accelerated. It is my opinion that future research with high copper HSLA-100 should include:

- Examination of a sample aged at a temperature between 538°C and 566°C to examine a possible increase in strength and toughness.
- Determination of the amount of carbon present in the retained austenite present at lath boundaries. Due to the size of the retained austenite, convergent beam electron diffraction (CBED) would probably be the best way to undertake this study
- Obtain continuous-cooling transformation (CCT) curves for the high copper HSLA-100 and measure the cooling rates of different quench treatments to enable exact correlation between cooling rate and microstructures. [Ref. 2:p. 79]
- The role and chemical composition of precipitated carbides involved in the strength and toughness mechanisms of high copper HSLA-100 steel. Statistical analysis may provide a better understanding on mechanical properties. [Ref. 18:p. 65]

APPENDIX

TABLE A-1. DTRC CHARPY V-NOTCH IMPACT ENERGY TEST DATA HIGH COPPER HSLA-100 DTRC CODE GLB: AS-QUENCHED CONDITION

SPECIMEN ID NO.	TEST TEMPERATURE (°F)	IMPACT ENERGY (FT*LBS)
9	ROOM TEMP	90
10	ROOM TEMP	84
11	ROOM TEMP	90
25	ROOM TEMP	72
26	ROOM TEMP	76
27	ROOM TEMP	744
12	0	91
13	0	91
14	0	87
28	0	69
29	0	70
30	0	70
15	-40	83
16	-40	87
17	-40	83
31	-40	69
32	-40	67
33	-40	70
18	-80	77
19	-80	77
20	-80	79
34	-80	61
35	-80	66
36	-80	63
21	-120	68
22	-120	70
23	-120	74
37	-120	58
38	-120	55
39	-120	54

TABLE A-2. DTRC CHARPY V-NOTCH IMPACT ENERGY TEST DATA HIGH COPPER HSLA-100 DTRC CODE GLB: AGING TEMPERATURE 538°C

SPECIMEN ID NO.	TEST TEMPERATURE (°F)	IMPACT ENERGY (FT*LBS)
13	ROOM TEMP	84
14	ROOM TEMP	84
15	ROOM TEMP	83
16	0	72
17	0	71
18	0	68
19	-40	56
20	-40	58
21	-40	56
22	-80	40
23	-80	45
24	-80	48
25	-120	35
26	-120	35
27	-120	48

TABLE A-3. DTRC CHARPY V-NOTCH IMPACT ENERGY TEST DATA HIGH COPPER HSLA-100 DTRC CODE GLB: AGING TEMPERATURE 566°C

SPECIMEN ID NO.	TEST TEMPERATURE (°F)	IMPACT ENERGY (FT*LBS)
29	ROOM TEMP	88
30	ROOM TEMP	87
31	ROOM TEMP	93
32	0	78
33	0	82
34	0	69
35	-40	72
36	-40	76
37	-40	78
39	-80	53
40	-80	53
44	-80	68
41	-120	53
42	-120	64
43	-120	58

TABLE A-4. DTRC CHARPY V-NOTCH IMPACT ENERGY TEST DATA HIGH COPPER HSLA-100 DTRC CODE GLB: AGING TEMPERATURE 593°C

SPECIMEN ID NO.	TEST TEMPERATURE (°F)	IMPACT ENERGY (FT*LBS)
45	ROOM TEMP	109
46	ROOM TEMP	107
47	ROOM TEMP	83
48	0	99
49	0	100
50	0	103
51	-40	101
52	-40	104
53	-40	97
54	-80	81
55	-80	79
56	-80	86
57	-120	62
58	-120	62
59	-120	70

TABLE A-5. DTRC CHARPY V-NOTCH IMPACT ENERGY TEST DATA HIGH COPPER HSLA-100 DTRC CODE GLB: AGING TEMPERATURE 621°C

SPECIMEN ID NO.	TEST TEMPERATURE (°F)	IMPACT ENERGY (FT*LBS)
61	ROOM TEMP	113
62	ROOM TEMP	131
63	ROOM TEMP	119
64	0	115
65	0	130
66	0	113
67	-40	122
68	-40	117
69	-40	122
70	-80	114
71	-80	107
72	-80	106
73	-120	89
74	-120	74
75	-120	91

LIST OF REFERENCES

1. Czyrca, Ernest J., *Development of Low-Carbon, Copper-Strengthened HSLA Steel Plate for Naval Ship Construction,* DTRC-SME-90/21, June 1990.

2. Mohr, Thomas C., "A Study of the Microstructural Basis for the Strength and Toughness Properties of Water Quenched and Air Cooled HSLA-100, HSLA-100 with Increased Copper and a ULCB Steel," Master's Thesis, Naval Postgraduate School, Monterey, California, September 1991.

3. Gudas, John P., *Pre-certification Development Plan - HSLA-130 for Submarine Construction,* David Taylor Research Center, Metals and Welding Division, Annapolis, Maryland, March 1989.

4. Czyrca, Ernest J., R.E. Link, R.J. Wong, D.A. Aylor, T.W. Montemarano and J.P. Gudas, *Development and Certification of HSLA-100 Steel for Naval Ship Construction,* Naval Engineers Journal, May 1990.

5. Anderson, T.L., J.A. Hyatt, and J.C. West, "The Benefits of New High Strength Low-Alloy (HSLA) Steels," *Welding Journal,* Vol. 66, September 1987.

6. Irving, R.R., "Microalloying: The Route to Stronger, Tougher Steels," *Iron Age,* Vol. 226, no. 5, pp. 41-45, February 1983.

7. Comerford, L.W., "A Study of the Microstructural Basis for the Strength and Toughness Properties of the Overaged HSLA-100 Steel," Master's Thesis, Naval Postgraduate School, Monterey, California, June 1991.

8. Porter, L.F., and P.E. Repas, "The Evolution of HSLA Steels," *Journal of Metals,* pp. 14-21, April 1982.

9. Pickering, F.B., *Physical Metallurgy of the Design of Steels,* Applied Science Publishers, Ltd., London, 1978.

10. Bucher, J.H., E.G. Hamburg, and A.D. Wilson, *Symposium on Toughness Characterization and Specifications for HSLA and Structural Steels,* The Metallurgical Society of AIME, March 1977.

11. Coldren, A.P., and T.B. Cox, "Development of 100 Ksi Yield Strength HSLA Steel," DTNSRDC/SME-CR-07-86, July 1986.

12. Natishan, M.E., *Mechanisms of Strength and Toughness in a Microalloyed Precipitation Hardened Steel,* PhD Thesis, University of Virginia, 1989.

13. LeMay, I., and L.M. Schetky, *Copper in Iron and Steel,* John Wiley and Sons, New York.

14. Wilson, A.D., E.G. Hamburg, D.J. Calvin, S.W. Thompson, and G. Krauss, "Properties and Microstructures of Copper Precipitation Aged Plate Steels, Microalloyed HSLA Steels," *Proceedings of Microalloying '88,* ASM International, pp. 259-274.

15. Kiesling, R.K., *Non-Metallic Inclusions in Steel, Part V,* The Institute of Metals, London, 1978.

16. Hertzberg, R.W., *Deformation and Fracture Mechanics of Engineering Materials,* 3rd ed., John Wiley and Sons, Inc., 1989.

17. Ellis, D., *The Effects of Titanium Inclusions on HY-80 GMA Weld Deposits,* Master's Thesis, Naval Postgraduate School, Monterey, California, December 1990.

18. Mattes, V.R., "Microstructure and Mechanical Properties of HSLA-100 Steel," Master's Thesis, Naval Postgraduate School, Monterey, California, December 1990.

19. Richman, M.H., *An Introduction to the Science of Metals,* Ginn Custom Publishing, Massachusetts, 1974.

20. Miglin, M.T., and others, "Microstructure of a Quenched and Tempered Cu-Bearing High Strength Low Alloy Steel," *Metallurgical Transactions A,* Vol. 17A, May 1986.

21. Hornbogen, E., "Aging and Plastic Deformation of an Fe-0.9% Cu Alloy," *Transactions of ASM,* Vol. 57, 1964.

22. Dahmen, U., P. Ferguson, and K.H. Westmacott, "Invariant Line Strain and Needle-Precipitate Growth Directions in Fe-Cu," *Acta Mellurgica,* Vol. 32, no. 5, pp. 803-810, 1984.

23. Speich, G.R., and R.A. Orani, "The Rate of Coarsening of Copper Precipitate in an Alpha-Iron Matrix," *Transactions of the Metallurgical Society of AIME,* Vol. 233, April 1965.

24. Goodman, S.R., S.S. Brenner, and J.R. Low, *An FIM-Atom Probe Study of the Precipitation of Copper from Iron-1.4 At. Pct. Copper. Part I: Field-Ion Microscopy,* Metallurgical Transactions, Vol. 4, October 1973.

25. Goodman, S.R., S.S. Brenner, and J.R.. Low, *An FIM-Atom Probe Study of the Precipitation of Copper From Iron-1.4 at. Pct Copper. Part II: Atom Probe Analysis,* Metallurgical Transactions, Vol. 4, October 1973.

26. Hamburg, E.G., and A.D. Wilson, "Production and Properties of Copper Age-Hardened Steels," *Processing, Microstructure and Properties of HSLA Steels,* edited by A.J. De Ardo, The Minerals, Metals and Materials Society, 1988.

27. Kraus, G., "Principles of Heat Treatment of Steel," *American Society for Metals,* Metals Park, Ohio, 1980.

28. Christian, J.W., *The Theory of Transformations in Metals and Alloys,* Pergammon Press, Oxford, England, 1965.

29. Seal, A.K., and R.W.K. Honeycombe, "Carbide Precipitation in Several Steels Containing Chromium and Vanadium," *Journal of the Iron and Steel Institute,* January, 1958.

30. Reed-Hill, R.E., "Physical Metallurgy Principles," *P.W.S. Engineering,* Boston, Massachusetts, 1973.

31. Chilton, J.M. and P.M. Kelly, "The Strength of Ferrous Martensite," *Acta Metallurgica,* Vol. 16, May 1968.

32. Aborn, R.H., "Low Carbon Martensites," *Transactions of the ASM,* Vol. 48, 1956.

33. Speich, G.R., "Tempering of Low Carbon Martensite, *Transactions of Metallurgical Society of AIME,* Vol. 245, December 1969.

34. Payson, P. "Tempered Alloy Martensite," *Transactions of the ASM,* Vol. 51, 1959.

35. Lement, B.S., B.L. Averbach and M. Cohen, "Microstructural Changes on Tempering Iron-Carbon Alloys," *Transactions of the ASM,* Vol. 46, 1954.

36. Lement, B.S., B.L. Averbach and M. Cohen, "Further Study of Microstructural Changes on Tempering Iron-Carbon Alloys," *Transactions of the ASM,* Vol. 47, 1955.

37. Speich, G.R., "Tempered Ferrous Martensite Structures," *Metals Handbook,* Vol. 8, 8th Ed., American Society for Metals, Metals Park, Ohio.

38. Hirotsu, Y., and S. Nagakura, "Crystal Structure and Morphology of the Carbide Precipitated From Martensitic High Carbon Steel During the First Stage of Tempering, *Acta Metallurgica,* Vol. 20, April 1972.

39. Hirotsu, Y., and S. Nagakura, "Electron Microscopy and Diffraction Study of the Carbide Precipitated at the First Stage of Tempering of Martensitic Medium Carbon Steel," *Trans. JIM,* Vol. 15, 1974.

40. Mikalac, S., (DTRC Code 2814) Letter to LT Harvey A. Winters, Subject: Chemical Composition and Processing of HSLA-100 with Increased Copper Steel.

41. Sarikaya, G., G. Thomas, J.W. Steels, S.J. Barnard, and G.D.W. Smith, "Solute Element Partitioning and Austenite Stabilization in Steels," *International Conference on Solid-Solid Phase Transformations,* Hub Aronson, ed., 1982.

42. Howell, P.R., and R. Varughese, "Austenite Transformation Products in Quenched Low-Carbon HSLA Steel," *Proceedings,* XXII International Congress for Electron Microscopy, San Francisco, California, pp. 902-903, 1990.

INITIAL DISTRIBUTION LIST

		No. of Copies
1.	Defense Technical Information Center Cameron Station Alexandria, Virginia 22304-6145	2
2.	Library, Code 52 Naval Postgraduate School Monterey, California 93943-5002	2
3.	Department Chairman, Code ME/Hy Department of Mechanical Engineering Naval Postgraduate School Monterey, California 93943-5000	1
4.	Naval Engineering Curricular Office, Code 34 Naval Postgraduate School Monterey, California 93943-5000	1
5.	Professor A.G. Fox, Code ME/Fx Department of Mechanical Engineering Naval Postgraduate School Monterey, California 93943-5000	2
6.	Dr. M.G. Vassilaros, Code 2814 David Taylor Research Center Annapolis, Maryland 21402	2
7.	LT Harvey A. Winters 5230 Johnstown Lane Virginia Beach, Virginia 23464	2